mathematics

Article

On the Forced Vibration of Bending-Torsional-Warping Coupled Thin-Walled Beams Carrying Arbitrary Number of 3-DoF Spring-Damper-Mass Subsystems

Jun Chen and Xiang Liu *

Key Laboratory of Traffic Safety on Track of Ministry of Education, School of Traffic and Transportation Engineering, Central South University, Changsha 410075, China
* Correspondence: xiangliu@csu.edu.cn; Tel.: +86-138-7314-4366

Abstract: This paper presents an analytical transfer matrix modeling framework for the forced vibration of a bending-torsional-warping coupling Euler-Bernoulli thin-walled beam carrying an arbitrary number of three degree-of-freedom (DOF) spring-damper-mass (SDM) subsystems. The thin-walled beam is divided into a series of distinct sub-beams whose ends are connected to the SDM subsystems. The transfer matrix for each sub-beam is developed based on the exact shape functions of the bending-torsional-warping coupling Euler-Bernoulli theory. Each SDM system is modelled by a set of effective springs based on the dynamic condensation method. The governing matrix equation is formulated based on the compatibility conditions of the placement and the force at the common interfaces of two adjacent sub-beams. Then, a closed-form expression for the frequency response function of the thin-walled beam system is proposed. The results computed by the proposed method achieve good agreement with those obtained by the conventional finite-element method, which shows the accuracy and reliability of the proposed method. The effects of the system parameters on the vibration transmission and vibration isolation properties of the thin-walled beam system are studied. The presented method can simultaneously consider arbitrary number of SDM subsystems and boundary conditions. Furthermore, none of the associated matrices are larger than 12×12, which provides a significant computational advantage.

Keywords: thin-walled beams; spring-damper-mass subsystems; transfer matrix method; force vibration; frequency response function

MSC: 74 Mechanics of deformable solids

check for updates

Citation: Chen, J.; Liu, X. On the Forced Vibration of Bending-Torsional-Warping Coupled Thin-Walled Beams Carrying Arbitrary Number of 3-DoF Spring-Damper-Mass Subsystems. *Mathematics* **2022**, *10*, 2849. https://doi.org/10.3390/math10162849

Academic Editor: Andrey Amosov

Received: 14 July 2022
Accepted: 8 August 2022
Published: 10 August 2022

1. Introduction

Thin-walled structures are commonly found in most branches of structural engineering such as aircraft wings, vehicle bodies, ship-hull structures, wind-turbine towers, construction machinery arms and bridge decks. The inconsistency of the shear center and mass center leads to severe bending-torsional-warping coupling dynamic behaviors of the thin-walled structures. The evaluation of these dynamic behaviors of thin-walled structures has long been regarded as a significant task for designers in order to avoid dangerous resonance situations and improve dynamics performance and structural robustness.

A large numbers of researchers have made efforts to deal with the dynamic models of thin-walled structures. Narayanan et al. [1] investigated the free vibration characteristics of a thin-walled open section beam with unconstrained damping layers at the flanges. Bank and Kao [2] studied the forced and free vibration of a thin-walled composite material Timoshenko beam. Rao and Jin [3] proposed a universal grey number-based approach and an interval-discretization method to analyze the coupled bending-torsional vibration of thin-walled beams involving uncertainties. To give a more accurate description to the dynamic behavior of thin-walled structures, tarping is further considered in the modeling of thin-walled structures. Li et al. [4–6] employed the dynamic transfer matrix method to investigate the free and stochastic vibration of the bending-torsion of coupled thin-walled structures, and their method took the effect of warping stiffness into account and allowed the presence of axial force. Lezgy-Nazargah et al. [7] proposed a quasi-3D finite element model to study the coupled bending and torsional–warping dynamics of thin-walled beams. Jrad et al. [8] analytically study the free and forced vibration of warping and flexural–torsional coupling thin-walled beams and discussed the dynamic behavior of thin-walled beams in the design of buildings and bridges. Thin-walled structures with complex shape section were also extensively studied for practical applications. Based on the d'Alembert principle, Chen and Hsiao [9] derived the governing equations of the axial-torsional coupled vibration of thin-walled Z-section beam. Prokić [10,11] derived the governing differential equations for triply coupled and fivefold coupled vibration of thin-walled with arbitrary cross-section by using the principle of virtual displacements. Chen and Hsiao [12] presented a finite element formulation for the quadruply coupled vibration analysis of thin-walled beams with a generic open section. By introducing Vlasov's assumptions, Kim et al. [13,14] investigated the free vibration and spatial stability of the circular curved thin-walled beams with non-symmetric sections. Xu et al. [15] analyzed the high-order vibration modes of thin-walled beams with complex open cross-sections using the framework of Carrera Unified Formulation.

The studies in Refs. [1–15] concentrated on the dynamic behavior of uniform beams, with no attachments or subsystems mounted along the span. However, in engineering practice, thin-walled structures such as aircraft wings, vehicle bodies, ship-hulls and wind-turbine towers are often mounted with lumped mass oscillations. Hence, study of the dynamic behaviors of thin-walled structures with elastically mounted masses is desperately needed for the structural design of these systems. Many investigations have been focused on the dynamic behavior of classical Bernoulli-Euler and/or Timoshenko beams with single or multiple lumped masses, including the free vibration (beams with attachments [16–18], beams with single-degree of freedom SDM subsystems [19–23], beams with two-degree of freedom SDM subsystems [24–28]) and forced vibration (beams with attachments [17,29], beams with single-degree of freedom SDM subsystems [30–35], and beams with two-degree of freedom SDM subsystem [36,37]) dynamics. In general, for a large number of thin-walled beams used in practical engineering, the shear center and the mass centroid are not coincident, which results in a coupling of the bending and torsional modes of the oscillation that are independent in classical beams. Therefore, the coupled vibration between rigid motions of subsystems and thin-walled beams becomes more complicated than classical beams and needs to be clarified [38,39]. Oguamanam et al. studied the coupled flexural–torsional free vibration of thin-walled beams with tip mass attachments [38]. Gökdağ and Kopmaz [39] analyzed the influences of tip mass and distributed mass on the coupled bending and torsional free vibration characteristic of cantilever thin-walled beams with different cross sections. Wang et al. [40] investigated the natural frequencies and mode shapes of a thin-walled turbine tower with different elastic attachments, and in his model the variations of material and cross section are considered using D'Alembert's principle. Wu and Titurus [41] studied the damping enhancement of thin-walled a helicopter blades system by internally distributed spring-damper elements; in this research, the closed-form governing equation of the thin-walled systems are established by Lagrange's equation. Hoffmeyer and Høgsberg [42] studied the vibration absorber characteristic of multiple tuned mass absorbers acting on bending-torsion coupled thin-walled beams. In the above studies, the dimensions of the governing equations are increased with the number of subsystems, which result in a heavy burden of computation. By employing the complex modal analysis approach, Burlon et al. obtained the closed analytical solutions for the frequency response of bending-torsional-warping coupled thin-walled beams with arbitrary attached masses, springs [43–45], dampers [46] and sub-beams [47], and the free, forced and stochastic vibration dynamics of these models were systematically discussed. Furthermore, all of the associated matrices of their modal are less than 6 × 6, resulting in a significant computational advantage.

It is noticed, however, that, the solutions in [43–47] are unable to compute the frequency response of bending-torsional-warping coupled thin-walled beams with multiple DOF spring-damper-mass subsystems. Hance, closed analytical solutions for the bending-torsional-warping coupled frequency response of thin-walled beams with multiple DOF spring-damper-mass subsystems is significant for the parameter design of multiple DOF absorbance and elastic suspension in vibration reduction application. Furthermore, despite the valuable insights provided by transform methods [48,49], no analytical expressions are available for the bending-torsional-warping coupled frequency response of thin-walled beams with multiple DOF spring-damper-mass subsystems; this requires a specific complex transformation approach with dynamic condensation.

This paper presents a new closed analytical approach to obtaining the forced vibration of bending-torsional-warping coupled thin-walled beams with an arbitrary number of 3-DoF spring-damper-mass subsystems and boundary conditions, based on the transfer matrix approach and dynamic condensation methods. The size of all associated matrices is always less than 12 × 12 regardless of the number of subsystems, which leads to great computational efficiency. The results computed by the proposed method achieve good agreement with those obtained by the conventional finite-element method. The effects of the system parameters on the vibration transmission and vibration isolation properties of the thin-walled beam system are studied.

2. Derivation of the Frequency Response Function

Figure 1 illustrates the physical model of the thin-walled beam system under investigation, which consists of a bending-torsional coupled thin-walled beam with N three-degree-of-freedom spring-damper-mass systems attached to it. The whole beam is subdivided into $N + 1$ segments with length l_i ($i = 1,2 \cdots N + 1$) at the positions xi where ($i = 1,2 \cdots N$) the subsystems locate.

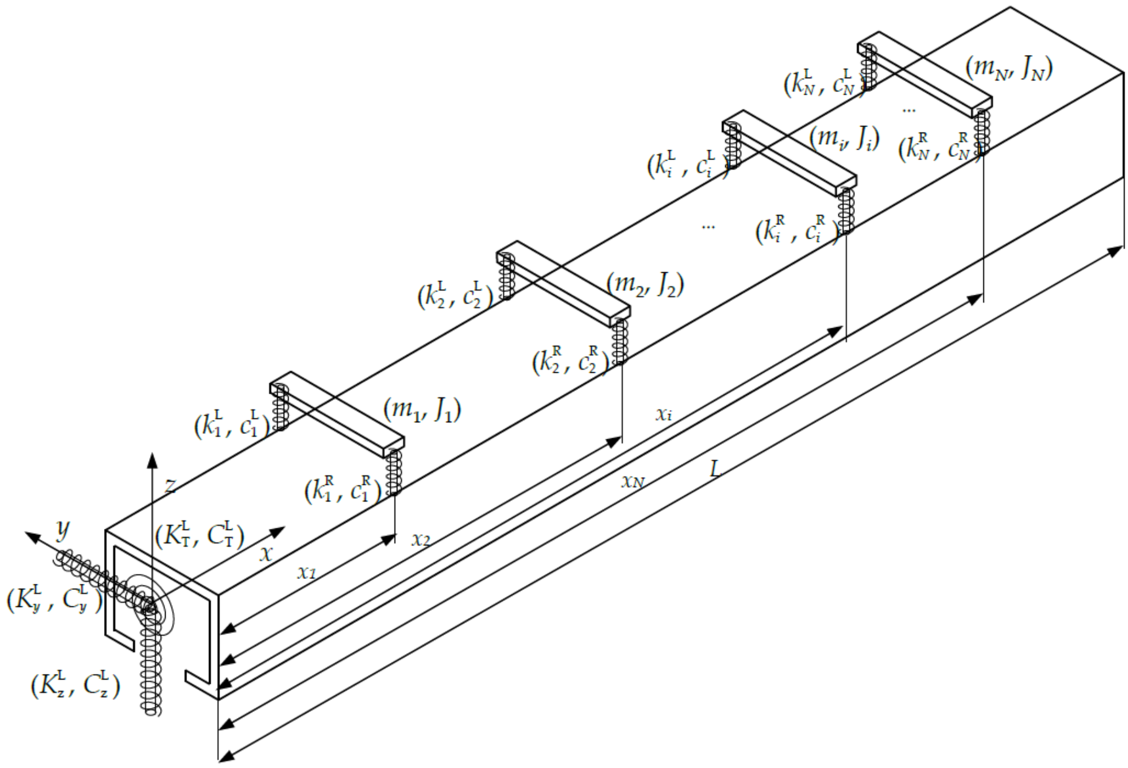

Figure 1. A elastically-damping constraint thin-walled beam carrying a number of spring-damper-mass systems.

The primary assumptions of the system are as follows: (a) the beam is a Euler-Bernoulli thin-walled beam with only the transverse in z and y directions and torsional vibration considered; (b) the cross-section is perfectly rigid in its own plane; (c) all the springs are idealized as general points connecting to the thin-walled beam.

Figure 2a illustrate the physical model for the cross section of the thin-walled beam system at the connection point. As shown in the figure, the variables are defined as follows: m_i the lumped mass; J_i the mass moment of inertia; $k_{z,i}^{\mathrm{L}}$, $k_{z,i}^{\mathrm{R}}$, $k_{y,i}^{\mathrm{L}}$, $k_{z,i}^{\mathrm{R}}$ and $c_{z,i}^{\mathrm{L}}$, $c_{z,i}^{\mathrm{R}}$, $c_{y,i}^{\mathrm{L}}$, $c_{z,i}^{\mathrm{R}}$ denote the stiffness and the damping of the left and right springs of the SDM system in z and y directions, respectively; l_i^{L} and l_i^{R} are the distance between the lumped mass and the left and right springs; y_i and θ_i, the translational displacement and the rotational angle of the lumped mass respectively; $v_{z,i}^{\mathrm{L}}$, $v_{z,i}^{\mathrm{R}}$, $v_{y,i}^{\mathrm{L}}$, and $v_{y,i}^{\mathrm{R}}$ the transverse displacements of the beam in z and y directions at the node connected with the two springs, respectively; $u_{z,i}^{\mathrm{L}}$, $u_{z,i}^{\mathrm{R}}$, $u_{y,i}^{\mathrm{L}}$, and $u_{y,i}^{\mathrm{R}}$ denote the corresponding displacements of the lump mass. S and C are the shearing center and mass center of the cross section, respectively. v_{i} and w_i denote the displacement in z and y direction of the thin-walled beam, ψ_i is rotational displacement in x direction. z_{c} is the distance between S and C. a and b is the length and wide of the cross section.

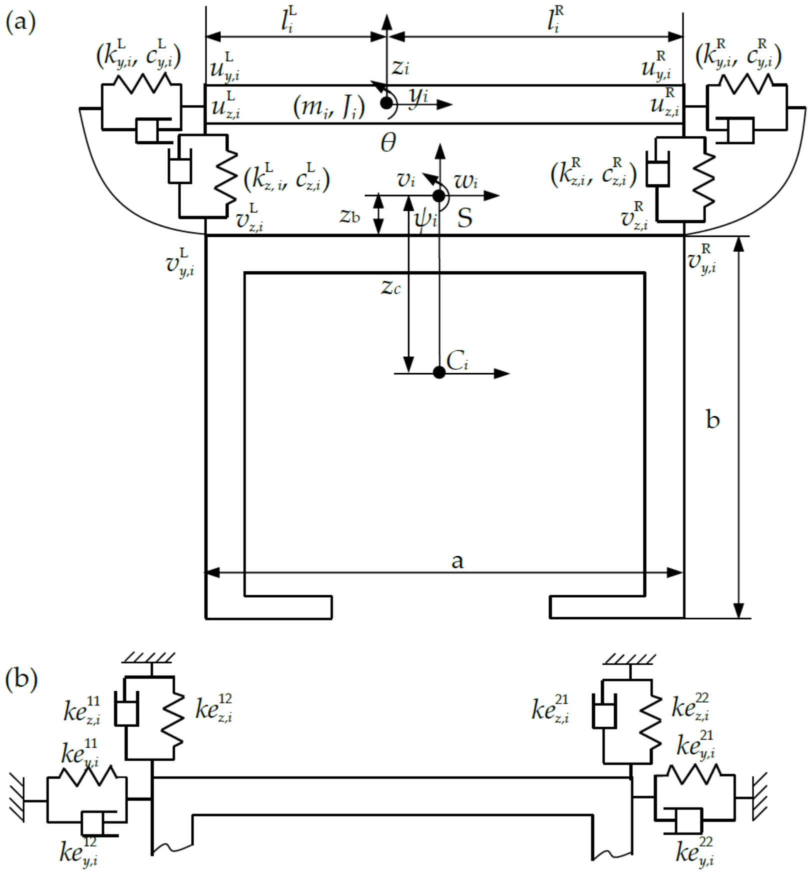

Figure 2. (**a**) The cross section of the thin-walled beam system at the connection point; (**b**) the three-DOF SDM subsystems is condensed into eight complex effective stiffness via dynamic condensation.

2.1. Dynamic Condensation of the Three-DOF SDM Subsystems

The internal force of springs $k_{y,i}^{\mathrm{L}}$, $k_{y,i}^{\mathrm{R}}$, $k_{z,i}^{\mathrm{L}}$ and $k_{z,i}^{\mathrm{R}}$ can be reasonably given as

$$F_{y,i}^{\mathrm{L}} = ke_{y,i}^{11} v_{y,i}^{\mathrm{L}} + ke_{y,i}^{12} v_{y,i}^{\mathrm{R}} \quad F_{y,i}^{\mathrm{R}} = ke_{y,i}^{21} v_{y,i}^{\mathrm{L}} + ke_{y,i}^{22} v_{y,i}^{\mathrm{R}} \tag{1}$$

$$F_{z,i}^{\mathrm{L}} = ke_{z,i}^{11} v_{z,i}^{\mathrm{L}} + ke_{z,i}^{12} v_{z,i}^{\mathrm{R}} \quad F_{z,i}^{\mathrm{R}} = ke_{z,i}^{21} v_{z,i}^{\mathrm{L}} + ke_{z,i}^{22} v_{z,i}^{\mathrm{R}} \tag{2}$$

where

$$ke_{y,i}^{11} = \frac{(-m_i\overline{\omega}^2 - \overline{\omega}c_{y,i}^{\mathrm{R}} - k_{y,i}^{\mathrm{R}})(\overline{\omega}c_{y,i}^{\mathrm{L}} + k_{y,i}^{\mathrm{L}})}{m_i\overline{\omega}^2 + \overline{\omega}(c_{y,i}^{\mathrm{L}} + c_{y,i}^{\mathrm{R}}) + (k_{y,i}^{\mathrm{L}} + k_{y,i}^{\mathrm{R}})} \tag{3}$$

$$ke_{y,i}^{12} = \frac{(\overline{\omega}c_{y,i}^{\mathrm{R}} + k_{y,i}^{\mathrm{R}})(\overline{\omega}c_{y,i}^{\mathrm{L}} + k_{y,i}^{\mathrm{L}})}{m_i\overline{\omega}^2 + \overline{\omega}(c_{y,i}^{\mathrm{L}} + c_{y,i}^{\mathrm{R}}) + (k_{y,i}^{\mathrm{L}} + k_{y,i}^{\mathrm{R}})} \tag{4}$$

$$ke_{y,i}^{21} = \frac{(\overline{\omega}c_{y,i}^{\mathrm{L}} + k_{y,i}^{\mathrm{L}})(\overline{\omega}c_{y,i}^{\mathrm{R}} + k_{y,i}^{\mathrm{R}})}{m_i\overline{\omega}^2 + \overline{\omega}(c_{y,i}^{\mathrm{L}} + c_{y,i}^{\mathrm{R}}) + (k_{y,i}^{\mathrm{L}} + k_{y,i}^{\mathrm{R}})} \tag{5}$$

$$ke_{y,i}^{22} = \frac{(-m_i\overline{\omega}^2 - \overline{\omega}c_{y,i}^{\mathrm{L}} - k_{y,i}^{\mathrm{L}})(\overline{\omega}c_{y,i}^{\mathrm{R}} + k_{y,i}^{\mathrm{R}})}{m_i\overline{\omega}^2 + \overline{\omega}(c_{y,i}^{\mathrm{L}} + c_{y,i}^{\mathrm{R}}) + (k_{y,i}^{\mathrm{L}} + k_{y,i}^{\mathrm{R}})} \tag{6}$$

$$ke_{z,i}^{11} = W_{11}{X_1}^2 - W_{12}l_i^{\mathrm{L}}{X_1}^2 - W_{21}l_i^{\mathrm{L}}{X_1}^2 + W_{22}l_i^{\mathrm{L}2}{X_1}^2 - X_1 \tag{7}$$

$$ke_{z,i}^{12} = W_{11}X_1X_2 + W_{12}l_i^{\mathrm{R}}X_1X_2 - W_{21}l_i^{\mathrm{R}}X_1X_2 - W_{22}l_i^{\mathrm{L}}l_i^{\mathrm{R}}X_1X_2 \tag{8}$$

$$ke_{z,i}^{21} = W_{11}X_1X_2 - W_{12}l_i^{\mathrm{L}}X_1X_2 + W_{21}l_i^{\mathrm{L}}X_1X_2 - W_{22}l_i^{\mathrm{L}}l_i^{\mathrm{R}}X_1X_2 \tag{9}$$

$$ke_{z,i}^{22} = W_{11}{X_2}^2 + W_{12}l_i^{\mathrm{R}}{X_2}^2 + W_{21}l_i^{\mathrm{R}}{X_2}^2 + W_{22}l_i^{\mathrm{R}2}{X_2}^2 - X_2 \tag{10}$$

and

$$X_1 = k_{z,i}^{\mathrm{L}} + \overline{\omega}c_{z,i}^{\mathrm{L}}\ X_2 = k_{z,i}^{\mathrm{R}} + \overline{\omega}c_{z,i}^{\mathrm{R}}$$

$$\begin{aligned}
W_{11} &= \left[\begin{array}{l} J_i\overline{\omega}^2 + \overline{\omega}(c_{z,i}^{\mathrm{L}}{l_{z,i}^{\mathrm{L}}}^2 + c_{z,i}^{\mathrm{R}}{l_{z,i}^{\mathrm{R}}}^2) \\ +(k_{z,i}^{\mathrm{L}}{l_{z,i}^{\mathrm{L}}}^2 + k_{z,i}^{\mathrm{R}}{l_{z,i}^{\mathrm{R}}}^2) \end{array}\right]/\Delta \\
W_{12} &= \left[(k_{z,i}^{\mathrm{L}}l_{z,i}^{\mathrm{L}} - k_{z,i}^{\mathrm{R}}l_{z,i}^{\mathrm{R}}) + \overline{\omega}(c_{z,i}^{\mathrm{L}}l_{z,i}^{\mathrm{L}} - c_{z,i}^{\mathrm{R}}l_{z,i}^{\mathrm{R}})\right]/\Delta = W_{21} \\
W_{22} &= \left[m_i\overline{\omega}^2 + \overline{\omega}(c_{z,i}^{\mathrm{L}} + c_{z,i}^{\mathrm{R}}) + (k_{z,i}^{\mathrm{L}} + k_{z,i}^{\mathrm{R}})\right]/\Delta
\end{aligned}$$

with

$$\Delta = \begin{vmatrix} m_i\overline{\omega}^2 + \overline{\omega}(c_{z,i}^{\mathrm{L}} + c_{z,i}^{\mathrm{R}}) + (k_{z,i}^{\mathrm{L}} + k_{z,i}^{\mathrm{R}}) & -(k_{z,i}^{\mathrm{L}}l_{z,i}^{\mathrm{L}} - k_{z,i}^{\mathrm{R}}l_{z,i}^{\mathrm{R}}) - \overline{\omega}(c_{z,i}^{\mathrm{L}}l_{z,i}^{\mathrm{L}} - c_{z,i}^{\mathrm{R}}l_{z,i}^{\mathrm{R}}) \\ -(k_{z,i}^{\mathrm{L}}l_{z,i}^{\mathrm{L}} - k_{z,i}^{\mathrm{R}}l_{z,i}^{\mathrm{R}}) - \overline{\omega}(c_{z,i}^{\mathrm{L}}l_{z,i}^{\mathrm{L}} - c_{z,i}^{\mathrm{R}}l_{z,i}^{\mathrm{R}}) & J_i\overline{\omega}^2 + \overline{\omega}(c_{z,i}^{\mathrm{L}}{l_{z,i}^{\mathrm{L}}}^2 + c_{z,i}^{\mathrm{R}}{l_{z,i}^{\mathrm{R}}}^2) + (c_{z,i}^{\mathrm{L}}{l_{z,i}^{\mathrm{L}}}^2 + c_{z,i}^{\mathrm{R}}{l_{z,i}^{\mathrm{R}}}^2) \end{vmatrix}$$

From Equations (1) and (2), one can see that the four springs, four dampers, lumped mass and mass movement of inertia of the three-DOF SDM system (see Figure 2a) are, respectively, condensed into eight effective springs $ke_{z,i}^{11}$, $ke_{z,i}^{12}$, $ke_{y,i}^{21}$, $ke_{y,i}^{22}$ and $ke_{z,i}^{11}$, $ke_{z,i}^{12}$, $ke_{y,i}^{21}$, $ke_{y,i}^{22}$ as shown in Figure 2b; the derivations of Equations (1)–(10) are given in Appendix A.

2.2. The Frequency Response Function for the Thin-Walled Beam System

The governing equations of motion of Euler-Bernoulli thin-walled beams illustrated in Figure 2a on which the external loads is zero can be written as follows:

$$EI_z\frac{\partial^4 v}{\partial x^4} + \rho A\frac{\partial^2 v}{\partial t^2} = 0 \tag{11}$$

$$EI_y\frac{\partial^4 w}{\partial x^4} + \rho A\frac{\partial^2 w}{\partial t^2} + \rho Az_c\frac{\partial^2 \psi}{\partial t^2} = 0 \tag{12}$$

$$E\Gamma_0\frac{\partial^4 \psi}{\partial x^4} - GJ\frac{\partial^2 \psi}{\partial x^2} + \rho Az_c\frac{\partial^2 w}{\partial t^2} + \rho I_0\frac{\partial^2 \psi}{\partial t^2} = 0 \tag{13}$$

where E is Young's modulus of elasticity and G is the shear modulus of the material, EI_z and EI_y are the bending stiffness of the thin-walled beam about the centroidal principal axes, which are parallel to the y and z axes, respectively. GJ and $E\Gamma_0$ are, respectively, the torsional stiffness and warping stiffness of the thin-walled beam. ρA is the mass of the thin-walled beam per unit length and I_0 denotes the polar mass moment of inertia of per unit length beam cross section about the x axis.

For forced vibration of the constrained thin-walled beam (beam with subsystems), the harmonic responses take the form:

$$v = V(x)e^{\overline{\omega}t} \; w = W(x)e^{\overline{\omega}t} \; \psi = \Psi(x)e^{\overline{\omega}t} \tag{14}$$

where $\overline{\omega} = \Omega\bar{i}$ is the frequency of the excitation force and $\bar{i} = \sqrt{-1}$.

Substituting Equation (14) into Equations (11)–(13) yields

$$EI_z V^{(4)}(x) + \rho A\overline{\omega}^2 V(x) = 0 \tag{15}$$

$$EI_y W^{(4)}(x) + \rho A\overline{\omega}^2 W(x) + \rho A z_c\overline{\omega}^2\Psi(x) = 0 \tag{16}$$

$$E\Gamma_0\Psi^{(4)}(x) - GJ\Psi^{(2)}(x) + \rho A z_c\overline{\omega}^2 W(x) + \rho I_0\overline{\omega}^2\Psi(x) = 0 \tag{17}$$

From Equation (16):

$$\Psi(x) = -\frac{EI_y}{\rho A z_c\overline{\omega}^2}W^{(4)}(x) - \frac{1}{z_c}W(x) \tag{18}$$

Substituting Equation (18) into Equation (17) yields:

$$\left\{\lambda_4 D^8 + \lambda_3 D^6 + \lambda_2 D^4 + \lambda_1 D^2 + \lambda_0\right\} W(x) = 0 \tag{19}$$

where

$$\begin{array}{l} D = d/dx \; \lambda_4 = E^2\Gamma_0 I_y \; \lambda_3 = -GJEI_y \; \lambda_2 = E\Gamma_0\rho A\overline{\omega}^2 + \rho I_0\overline{\omega}^2 EI_y \\ \lambda_1 = -GJ\rho A\overline{\omega}^2 \; \lambda_0 = -(\rho A z_c\overline{\omega}^2)^2 + \rho^2 I_0 A\overline{\omega}^4 \end{array}$$

The solution of Equation (19) can be obtained by substituting the trial solution $W(x) = w_0 e^{\kappa x}$ to give the characteristic equation

$$\lambda_4\kappa^8 + \lambda_3\kappa^6 + \lambda_2\kappa^4 + \lambda_1\kappa^2 + \lambda_0 = 0 \tag{20}$$

Let h = κ^2, the Equation (20) can be rewritten as

$$\lambda_4 h^4 + \lambda_3 h^3 + \lambda_2 h^2 + \lambda_1 h^1 + \lambda_0 = 0 \tag{21}$$

For Equation (21), all of its four roots are real when the vibration frequency is within the practical range [4,5], two of them are positive (h_1 and h_2) and the other two are negative ($-h_3$ and $-h_4$). Then the eight roots of the characteristic Equation (21) are β_1, $-\beta_1$, β_2, $-\beta_2$, $\beta_3\bar{i}$, $-\beta_3\bar{i}$, $\beta_4 i$, $-\beta_4\bar{i}$, where $\bar{i} = \sqrt{-1}$ and $\beta_1 = \sqrt{h_1}$, $\beta_2 = \sqrt{h_2}$, $\beta_3 = \sqrt{-h_3}$, $\beta_4 = \sqrt{-h_4}$. It follows that the solutions of Equations (15)–(17) are in the following forms:

$$V(x) = c_9\sin\beta_5 x + c_{10}\cos\beta_5 x + c_{11}\mathrm{sinh}\beta_5 x + c_{12}\cosh\beta_5 x \tag{22}$$

$$W(x) = c_1\mathrm{sinh}\beta_1 x + c_2\cosh\beta_1 x + c_3\mathrm{sinh}\beta_2 x + c_4\cosh\beta_2 x + c_5\mathrm{sinh}\beta_3 x + c_6\cosh\beta_3 x + c_7\mathrm{sinh}\beta_4 x + c_8\cosh\beta_4 x \tag{23}$$

$$\Psi(x) = t_1 c_1\mathrm{sinh}\beta_1 x + t_1 c_2\cosh\beta_1 x + t_2 c_3\mathrm{sinh}\beta_2 x + t_2 c_4\cosh\beta_2 x + t_3 c_5\mathrm{sinh}\beta_3 x + t_3 c_6\cosh\beta_3 x + t_4 c_7\mathrm{sinh}\beta_4 x + t_4 c_8\cosh\beta_4 x \tag{24}$$

where ${\beta_5}^4 = \frac{\rho A}{EI_z}\overline{\omega}^2$ and c_1 to c_{12} is a set of constants, and

$$\begin{array}{l} t_1 = -(EI_y{\beta_1}^4 + \rho A\overline{\omega}^2)/\rho A z_c\overline{\omega}^2 \;\; t_2 = -(EI_y{\beta_2}^4 + \rho A\overline{\omega}^2)/\rho A z_c\overline{\omega}^2 \\ t_3 = -(EI_y{\beta_3}^4 + \rho A\overline{\omega}^2)/\rho A z_c\overline{\omega}^2 \;\; t_4 = -(EI_y{\beta_4}^4 + \rho A\overline{\omega}^2)/\rho A z_c\overline{\omega}^2 \end{array}$$

Following the sign convention as shown in Figure 2, the expressions of bending moment $M(x)$, shear force $S(x)$, torque $T(x)$ and bi-moment $B(x)$ can be obtained as

$$\begin{aligned} M^v(x) &= EI_z V''(x) = EI_z {\beta_5}^2(-c_9 \sin\beta_5 x - c_{10}\cos\beta_5 x + c_{11}\sinh\beta_5 x + c_{12}\cosh\beta_5 x) \\ M^w(x) &= EI_y W''(x) = EI_y(c_1{\beta_1}^2\sinh\beta_1 x + c_2{\beta_1}^2\cosh\beta_1 x + c_3{\beta_2}^2\sinh\beta_2 x + c_4{\beta_2}^2\cosh\beta_2 x \\ &\quad + c_5{\beta_3}^2\sinh\beta_3 x + c_6{\beta_3}^2\cosh\beta_3 x + c_7{\beta_4}^2\sinh\beta_4 x + c_8{\beta_4}^2\cosh\beta_4 x) \end{aligned} \tag{25}$$

$$\begin{aligned} S^v(x) &= EI_z V'''(x) = EI_z {\beta_5}^3(-c_9 \cos\beta_5 x + c_{10}\sin\beta_5 x + c_{11}\cosh\beta_5 x + c_{12}\sinh\beta_5 x) \\ S^w(x) &= EI_y W'''(x) = EI_y(c_1{\beta_1}^3\cosh\beta_1 x + c_2{\beta_1}^3\sinh\beta_1 x + c_3{\beta_2}^3\cosh\beta_2 x + c_4{\beta_2}^3\sinh\beta_2 x \\ &\quad + c_5{\beta_3}^3\cosh\beta_3 x + c_6{\beta_3}^3\sinh\beta_3 x + c_7{\beta_4}^3\cosh\beta_4 x + c_8{\beta_4}^3\sinh\beta_4 x) \end{aligned} \tag{26}$$

$$\begin{aligned} T(x) &= E\Gamma_0\Psi'''(x) - GJ\Psi'(x) \\ &= E\Gamma_0(c_1{\beta_1}^3 t_1\cosh\beta_1 x + c_2{\beta_1}^3 t_1\sinh\beta_1 x + c_3{\beta_2}^3 t_2\cosh\beta_2 x + c_4{\beta_2}^3 t_2\sinh\beta_2 x \\ &\quad + c_5{\beta_3}^3 t_3\cosh\beta_3 x + c_6{\beta_3}^3 t_3\sinh\beta_3 x + c_7{\beta_4}^3 t_4\cosh\beta_4 x + c_8{\beta_4}^3 t_4\sinh\beta_4 x) \\ &\quad - GJ(t_1c_1\beta_1\cosh\beta_1 x + t_1c_2\beta_1\sinh\beta_1 x + t_2c_3\beta_2\cosh\beta_2 x + t_2c_4\beta_2\sinh\beta_2 x \\ &\quad + t_3c_5\beta_3\cosh\beta_3 x + t_3c_6\beta_3\sinh\beta_3 x + t_4c_7\beta_4\cosh\beta_4 x + t_4c_8\beta_4\sinh\beta_4 x) \end{aligned} \tag{27}$$

$$\begin{aligned} B(x) = E\Gamma_0\Psi''(x) &= E\Gamma_0(t_1c_1{\beta_1}^2\sinh\beta_1 x + t_1c_2{\beta_1}^2\cosh\beta_1 x + t_2c_3{\beta_2}^2\sinh\beta_2 x + t_2c_4{\beta_2}^2\cosh\beta_2 x \\ &\quad + t_3c_5{\beta_3}^2\sinh\beta_3 x + t_3c_6{\beta_3}^2\cosh\beta_3 x + t_4c_7{\beta_4}^2\sinh\beta_4 x + t_4c_8{\beta_4}^2\cosh\beta_4 x) \end{aligned} \tag{28}$$

The spatial solution of Equations (15)–(17) can be expressed in terms of both sinusoidal and hyperbolic terms, and can be written in vector form as

$$V(x) = \boldsymbol{V}(x)\boldsymbol{C}_i^v \; W(x) = \boldsymbol{W}(x)\boldsymbol{C}_i^w \; \Psi(x) = \boldsymbol{\Psi}(x)\boldsymbol{C}_i^\psi \tag{29}$$

where $\boldsymbol{C}_i^v$, $\boldsymbol{C}_i^w$, $\boldsymbol{C}_i^\Psi$ are column vector of integration constants associated with the sub-beam i. $\boldsymbol{V}(x)$, $\boldsymbol{W}(x)$, $\boldsymbol{\Psi}(x)$ are row vectors of mode shape terms. And

$$\boldsymbol{C}_i^v = [c_9\ c_{10}\ c_{11}\ c_{12}]^T \boldsymbol{C}_i^v = [c_9\ c_{10}\ c_{11}\ c_{12}]^T \boldsymbol{V}(x) = [\sin\beta_5 x\ \ \cos\beta_5 x\ \sinh\beta_5 x\ \ \cosh\beta_5 x]$$

$$\boldsymbol{W}(x) = [\sinh\beta_1 x\ \ \cosh\beta_1 x\ \sinh\beta_2 x\ \ \cosh\beta_2 x\ \ \sinh\beta_3 x\ \ \cosh\beta_3 x\ \sinh\beta_4 x\ \ \cosh\beta_4 x]$$

$$\boldsymbol{\Psi}(x) = [t_1\sinh\beta_1 x\ t_1\cosh\beta_1 x\ t_2\sinh\beta_2 x\ \ t_2\cosh\beta_2 x\ t_3\sinh\beta_3 x\ t_3\cosh\beta_3 x\ t_4\sinh\beta_4 x\ t_4\cosh\beta_4 x]$$

From Figure 2a, the relationship between the displacement of connection points and the shear center can be given as follows

$$v_{y,i}^L = w_i + z_b\psi_i \; v_{y,i}^R = w_i + z_b\psi_i \; v_{z,i}^L = v_i - y_u\psi_i \; v_{z,i}^R = v_i + y_u\psi_i \tag{30}$$

where z_b and $y_u = a/2$ are the distances between the shearing center and spring connection point in z direction and y direction, respectively.

Substituting Equation (30) into Equations (1) and (2), one can obtain

$$F_{y,i}^L = (ke_{y,i}^{11} + ke_{y,i}^{12})(w_i + z_b\psi_i) \; F_{y,i}^R = (ke_{y,i}^{21} + ke_{y,i}^{22})(w_i + z_b\psi_i) \tag{31}$$

$$F_{z,i}^L = (ke_{z,i}^{11} + ke_{z,i}^{12})v_i + (-ke_{z,i}^{11} + ke_{z,i}^{12})y_u\psi_i \; F_{z,i}^R = (ke_{z,i}^{21} + ke_{z,i}^{22})v_i + (-ke_{z,i}^{21} + ke_{z,i}^{22})y_u\psi_i \tag{32}$$

Then the external force and torque applied at the shear center can be written as

$$F_{y,i} = F_{y,i}^L + F_{y,i}^R = (ke_{y,i}^{11} + ke_{y,i}^{12} + ke_{y,i}^{21} + ke_{y,i}^{22})(w_i + z_b\psi_i) = \overline{K}y_i(w_i + z_b\psi_i) \tag{33}$$

$$F_{z,i} = F_{z,i}^L + F_{z,i}^R = (ke_{z,i}^{11} + ke_{z,i}^{12} + ke_{z,i}^{21} + ke_{z,i}^{22})v_i + (-ke_{z,i}^{11} + ke_{z,i}^{12} - ke_{z,i}^{21} + ke_{z,i}^{22})y_u\psi_i = \overline{K}z_i v_i + \hat{K}z_i y_u\psi_i \tag{34}$$

$$\begin{aligned} T_i &= T_{yi} + T_{zi} = (F_{y,i}^L + F_{y,i}^R)z_b - F_{z,i}^L y_u + F_{z,i}^R y_u \\ &= (ke_{y,i}^{11} + ke_{y,i}^{12} + ke_{y,i}^{21} + ke_{y,i}^{22})(w_i + z_b\psi_i)z_b + (-ke_{z,i}^{11} - ke_{z,i}^{12} + ke_{z,i}^{21} + ke_{z,i}^{22})v_i y_u + (ke_{z,i}^{11} - ke_{z,i}^{12} - ke_{z,i}^{21} + ke_{z,i}^{22}){y_u}^2\psi_i \\ &= \overline{K}y_i(w_i + z_b\psi_i)z_b + \widehat{K}z_i v_i y_u + \widetilde{K}z_i {y_u}^2\psi_i \end{aligned} \tag{35}$$

The continuity condition at the cross section where the subsystem mounts enforces that the displacements and slopes at the common interface of two adjacent sub-beams must be equal, hence

$$W_i(l_i) = W_{i+1}(0),\ V_i(l_i) = V_{i+1}(0)\ \Psi_i(l_i) = \Psi_i(0)\ W_i'(l_i) = W_{i+1}'(0),\ V_i'(l_i) = V_{i+1}'(0)\ \Psi_i'(l_i) = \Psi_i'(0) \tag{36}$$

Similarly, the moment, force, torque and bi-moment at interface must be equal to zero and the equilibrium conditions are illustrated in Figure 3. Hence, one can obtain:

$$M_i^w(l_i) = M_{i+1}^w(0)\ M_i^v(l_i) = M_{i+1}^v(0) \tag{37}$$

$$S_i^w(l_i) + F_{y,i} = S_{i+1}^w(0)\ S_i^v(l_i) + F_{z,i} = S_{i+1}^v(0) \tag{38}$$

$$T_i(l_i) + T_{Ti} = T_{i+1}(0) \tag{39}$$

$$B_i(l_i) = B_{i+1}(l_{i+1}) \tag{40}$$

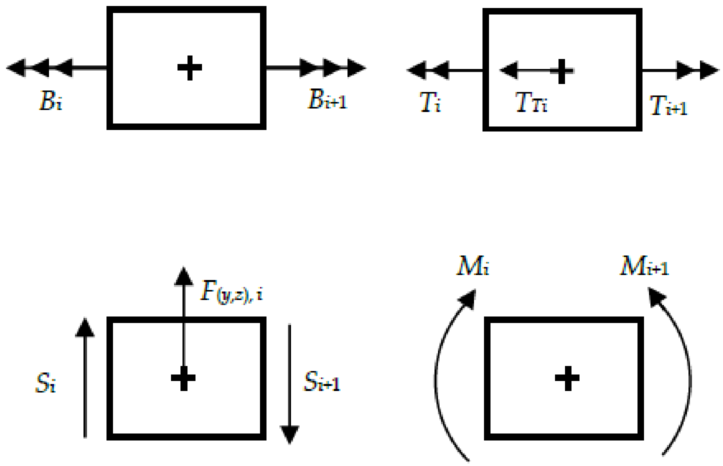

Figure 3. The force equilibrium conditions at the interface.

Substituting Equations (22)–(29) and (33)–(35) into Equations (36)–(40), and writing the compatibility conditions across the spring connection point in matrix form, one obtains

$$\mathbf{T}_{Ri}^w \boldsymbol{C}_{i+1}^w = \mathbf{T}_{Li}^w \boldsymbol{C}_i^w \tag{41}$$

$$\mathbf{T}_{Ri}^\psi \boldsymbol{C}_{i+1}^w = \mathbf{T}_{Li}^\psi \boldsymbol{C}_i^w + \mathbf{T}_{Li}^{\psi v} \boldsymbol{C}_i^v \tag{42}$$

$$\mathbf{T}_{Ri}^v \boldsymbol{C}_{i+1}^v = \mathbf{T}_{Li}^v \boldsymbol{C}_i^v + \mathbf{T}_{Li}^{v\psi} \boldsymbol{C}_i^\psi \tag{43}$$

where $\mathbf{T}^w$, $\mathbf{T}^\psi$ and $\mathbf{T}^v$ are the derivative matrices, the components of which are given in Appendix B.

Combining Equations (41)–(43) and organizing them in matrix form, one obtains

$$\underbrace{\begin{bmatrix} \mathbf{T}_{Ri}^w & 0_{4\times4} \\ \mathbf{T}_{Ri}^\psi & 0_{4\times4} \\ 0_{4\times8} & \mathbf{T}_{Ri}^v \end{bmatrix}}_{12\times12} \begin{bmatrix} \boldsymbol{C}_{i+1}^w \\ \boldsymbol{C}_{i+1}^v \end{bmatrix}_{12\times1} = \underbrace{\begin{bmatrix} \mathbf{T}_{Li}^w & 0_{4\times4} \\ \mathbf{T}_{Li}^\psi & \mathbf{T}_{Li}^{\psi v} \\ \mathbf{T}_{Li}^{v\psi} & \mathbf{T}_{Li}^v \end{bmatrix}}_{12\times12} \begin{bmatrix} \boldsymbol{C}_i^w \\ \boldsymbol{C}_i^v \end{bmatrix}_{12\times1} \tag{44}$$

Then, the transitive relationship between the integration constants of the ith and the i + 1th sub-beam is obtained:

$$\begin{bmatrix} \boldsymbol{C}_{i+1}^w \\ \boldsymbol{C}_{i+1}^v \end{bmatrix} = \begin{bmatrix} \mathbf{T}_{Ri}^w & 0_{4\times4} \\ \mathbf{T}_{Ri}^\psi & 0_{4\times4} \\ 0_{4\times8} & \mathbf{T}_{Ri}^v \end{bmatrix}^{-1} \begin{bmatrix} \mathbf{T}_{Li}^w & 0_{4\times4} \\ \mathbf{T}_{Li}^\psi & \mathbf{T}_{Li}^{\psi v} \\ \mathbf{T}_{Li}^{v\psi} & \mathbf{T}_{Li}^v \end{bmatrix} \begin{bmatrix} \boldsymbol{C}_i^w \\ \boldsymbol{C}_i^v \end{bmatrix} = \mathbf{H}_{i12\times12} \boldsymbol{C}_i \tag{45}$$

By repeating Equation (45), the transitive relationship between the first sub-beam and the last sub-beam can be written as

$$C_{N+1} = \left(\prod_{i=1}^{N} \mathbf{H}_{N-i+1}\right) C_1 = \mathbf{H}_{12\times 12} C_1 \tag{46}$$

where N is the total number of three-DOF SDM systems.

For the derivation of frequency response function of the thin-walled beam system, the basic idea is to treat the excitation force as an external discontinuity and involve it in the boundary or compatibility conditions associated with the shear force and torque of the thin walled beam.

2.2.1. Force Excitation at the Ends

Case 1. With a harmonic force ($F_{\mathrm{L}}^{\mathrm{w}} \mathrm{e}^{\mathrm{i}\Omega \mathrm{t}}$, $T_{\mathrm{L}}^{\psi} \mathrm{e}^{\mathrm{i}\Omega \mathrm{t}}$, $F_{\mathrm{L}}^{\mathrm{v}} \mathrm{e}^{\mathrm{i}\Omega \mathrm{t}}$) at the left-hand end of a thin-walled beam, the boundary conditions can be written as follows:

$$\underbrace{\begin{bmatrix} \mathbf{B}_{\mathrm{L}\,6\times 12} \\ \mathbf{B}_{\mathrm{R}\,6\times 12}\left(\prod_{i=1}^{N} \mathbf{H}_{N-i+1}\right) \end{bmatrix}}_{12\times 12} \begin{bmatrix} C_1^w \\ C_1^v \end{bmatrix} = \underbrace{\begin{bmatrix} F_{\mathrm{L}6\times 1} \\ 0_{6\times 1} \end{bmatrix}}_{12\times 1} = \bar{F}_{\mathrm{L}} \tag{47}$$

where $\bar{F}_{\mathrm{L}}$ = $[0\ F_{\mathrm{L}}^{w}\ 0\ T_{\mathrm{L}}^{\psi}\ 0\ F_{\mathrm{L}}^{v}\ 0\ 0\ 0\ 0\ 0\ 0]^T$ is excitation force vector; $\mathbf{B}_{\mathrm{L}}$ and $\mathbf{B}_{\mathrm{R}}$ are the coefficient matrices associated with the left and right ends; the expressions of these matrices are given in Appendix C. For any other boundaries, the boundary constraint equations are all in the form of Equation (47). Through changing the elements of matrices $\mathbf{B}_{\mathrm{L}}$, $\mathbf{B}_{\mathrm{R}}$, one can formulate the constraint equation for arbitrary boundary conditions easily.

By substituting Equation (46) into Equation (47), the integration constant parameters for the first component can be obtained as

$$[C_1] = \begin{bmatrix} C_1^w \\ C_1^v \end{bmatrix} = \underbrace{\begin{bmatrix} \mathbf{B}_{\mathrm{L}\,6\times 12} \\ \mathbf{B}_{\mathrm{R}\,6\times 12}\left(\prod_{i=1}^{N} \mathbf{H}_{N-i+1}\right) \end{bmatrix}}_{12\times 12}^{-1} \bar{F}_{\mathrm{L}} \tag{48}$$

Next, introducing Equation (48) into Equation (31) lead to the constant parameters for the nth sub-beam $\mathbf{C}_n$ and the corresponding FRFs can be expressed as [28]:

$$Y(\bar{x}) = \sum_{n=1}^{N+1} \mathbf{\Psi}_n(\bar{x}-\bar{x}_{n-1})\mathbf{C}_n[H(\bar{x}-\bar{x}_{n-1}) - H(\bar{x}-\bar{x}_n)] \tag{49}$$

where $\bar{x}$ is the global coordinate with $\bar{x}_0 = 0$ and $\bar{x}_{N+1} = L$, $H(\bar{x}-x_0)$ is the Heaviside function, which increases from zero to unity at location $x_{0.}$

Case 2. With a harmonic force ($\mathrm{F}_{\mathrm{R}}^{\mathrm{w}} \mathrm{e}^{\mathrm{i}\Omega \mathrm{t}}$, $\mathrm{T}_{\mathrm{R}}^{\psi} \mathrm{e}^{\mathrm{i}\Omega \mathrm{t}}$, $\mathrm{F}_{\mathrm{R}}^{\mathrm{v}} \mathrm{e}^{\mathrm{i}\Omega \mathrm{t}}$) applied at the right-hand end of the thin-walled beam, through similar matrix manipulations as in Equation (47), the integration constant parameters of the first sub-beam are

$$[C_1] = \begin{bmatrix} C_1^w \\ C_1^v \end{bmatrix} = \underbrace{\begin{bmatrix} \mathbf{B}_{\mathrm{L}\,6\times 12} \\ \mathbf{B}_{\mathrm{R}\,6\times 12}\left(\prod_{i=1}^{N} \mathbf{H}_{N-i+1}\right) \end{bmatrix}}_{12\times 12}^{-1} \bar{F}_{\mathrm{R}} \tag{50}$$

where $\bar{F}_{\mathrm{R}}$ = $[\ 0\ 0\ 0\ 0\ 0\ 0\ 0\ F_{\mathrm{R}}^{w}\ 0\ T_{\mathrm{R}}^{\psi}\ 0\ F_{\mathrm{R}}^{v}]^T$. Similarly, the FRFs can be expressed as Equation (49).

2.2.2. Force Excitation at an Arbitrary Position of the Thin-Walled Beam

In most conditions, the excitation force $F_u e^{i\Omega t}$ is applied at arbitrary positions of the system. The force equilibrium conditions at the excitation point of the mth sub-beam are illustrated in Figure 3 and can be written as

$$\mathbf{T}^{w}_{m,2}\boldsymbol{C}^{w}_{m,2} = \mathbf{T}^{w}_{m,1}\boldsymbol{C}^{w}_{m,1} + \boldsymbol{F}^{w} \tag{51}$$

$$\mathbf{T}^{\psi}_{m,2}\boldsymbol{C}^{w}_{m,2} = \mathbf{T}^{\psi}_{m,1}\boldsymbol{C}^{w}_{m,1} + \mathbf{T}^{\psi} \tag{52}$$

$$\mathbf{T}^{v}_{m,2}\boldsymbol{C}^{v}_{m,2} = \mathbf{T}^{v}_{m,1}\boldsymbol{C}^{v}_{m,1} + \boldsymbol{F}^{v} \tag{53}$$

where the subscripts (m, 1) and (m, 2) correspond to the 1th (left) and 2th (right) component of the mth sub-beam; $\boldsymbol{F}^w$= $[0\ 0\ 0\ F^w]^T$, $\boldsymbol{T}^\psi$= $[0\ 0\ 0\ T^\psi]^T$, $\boldsymbol{F}^v$= $[0\ 0\ 0\ F^v]^T$. the components of the derivative matrices are given in Appendix D.

The combination of Equations (51)–(53) leads to

$$\underbrace{\begin{bmatrix} \mathbf{T}^{w,1}_{m,2} & 0_{4\times4} \\ \mathbf{T}^{\psi,1}_{m,2} & 0_{4\times4} \\ 0_{4\times8} & \mathbf{T}^{v,1}_{m,2} \end{bmatrix}}_{12\times12} \begin{bmatrix} \boldsymbol{C}^{w}_{m,2} \\ \boldsymbol{C}^{v}_{m,2} \end{bmatrix}_{8\times1} = \underbrace{\begin{bmatrix} \mathbf{T}^{w,2}_{m,1} & 0_{4\times4} \\ \mathbf{T}^{\psi,2}_{m,1} & 0_{4\times4} \\ 0_{4\times8} & \mathbf{T}^{v,2}_{m,1} \end{bmatrix}}_{12\times12} \begin{bmatrix} \boldsymbol{C}^{w}_{m,1} \\ \boldsymbol{C}^{v}_{m,1} \end{bmatrix}_{8\times1} + \begin{bmatrix} \boldsymbol{F}^{w} \\ \mathbf{T}^{\psi} \\ \boldsymbol{F}^{v} \end{bmatrix} \tag{54}$$

Then, the transitive relationship between the integration constants of the 1th and the 2th component of the mth sub-beam is obtained:

$$\begin{bmatrix} \boldsymbol{C}^{w}_{m,2} \\ \boldsymbol{C}^{v}_{m,2} \end{bmatrix} = \begin{bmatrix} \mathbf{T}^{w,1}_{m,2} & 0_{4\times4} \\ \mathbf{T}^{\psi,1}_{m,2} & 0_{4\times4} \\ 0_{4\times8} & \mathbf{T}^{v,1}_{m,2} \end{bmatrix}^{-1} \begin{bmatrix} \mathbf{T}^{w,2}_{m,1} & 0_{4\times4} \\ \mathbf{T}^{\psi,2}_{m,1} & 0_{4\times4} \\ 0_{4\times8} & \mathbf{T}^{v,2}_{m,1} \end{bmatrix} \begin{bmatrix} \boldsymbol{C}^{w}_{m,1} \\ \boldsymbol{C}^{v}_{m,1} \end{bmatrix} + \begin{bmatrix} \mathbf{T}^{w,1}_{m,2} & 0_{4\times4} \\ \mathbf{T}^{\psi,1}_{m,2} & 0_{4\times4} \\ 0_{4\times8} & \mathbf{T}^{v,1}_{m,2} \end{bmatrix}^{-1} \begin{bmatrix} \boldsymbol{F}^{w} \\ \mathbf{T}^{\psi} \\ \boldsymbol{F}^{v} \end{bmatrix} = \hat{\mathbf{H}}_m \begin{bmatrix} \boldsymbol{C}^{w}_{m,1} \\ \boldsymbol{C}^{v}_{m,1} \end{bmatrix} + \mathbf{H}_F\hat{\boldsymbol{F}} \tag{55}$$

Case 1. *m* = *1*

The substitution of Equation (55) into Equation (46) leads to

$$\begin{bmatrix} \boldsymbol{C}^{w}_{N+1} \\ \boldsymbol{C}^{v}_{N+1} \end{bmatrix} = \left(\prod_{i=1}^{N} \mathbf{H}_{N-i+1}\right)\hat{\mathbf{H}}_1 \begin{bmatrix} \boldsymbol{C}^{w}_{1} \\ \boldsymbol{C}^{v}_{1} \end{bmatrix} + \left(\prod_{i=1}^{N} \mathbf{H}_{N-i+1}\right)\mathbf{H}_F\hat{\boldsymbol{F}} \tag{56}$$

Then the boundary conditions can be written as follows:

$$\underbrace{\begin{bmatrix} \mathbf{B}_{\mathrm{L}\,6\times12} \\ \mathbf{B}_{\mathrm{R}\,6\times12}\left(\prod\limits_{i=1}^{N} \mathbf{H}_{N-i+1}\right)\hat{\mathbf{H}}_1 \end{bmatrix}}_{12\times12} \begin{bmatrix} \boldsymbol{C}^{w}_{1} \\ \boldsymbol{C}^{v}_{1} \end{bmatrix} = \begin{bmatrix} 0 \\ -\mathbf{B}_{\mathrm{R}}\left(\prod\limits_{i=1}^{N} \mathbf{H}_{N-i+1}\right)\mathbf{H}_F\hat{\boldsymbol{F}} \end{bmatrix} = \overline{\boldsymbol{F}} \tag{57}$$

Next, the integration constant parameters of the first sub-beam can be written as

$$\begin{bmatrix} \boldsymbol{C}^{w}_{1} \\ \boldsymbol{C}^{v}_{1} \end{bmatrix} = \begin{bmatrix} \mathbf{B}_{\mathrm{L}\,6\times12} \\ \mathbf{B}_{\mathrm{L}\,6\times12}\left(\prod\limits_{i=1}^{N} \mathbf{H}_{N-i+1}\right)\hat{\mathbf{H}}_m \end{bmatrix}^{-1} \overline{\boldsymbol{F}} \tag{58}$$

Therefore, the integration constants of the $n+1$ ($n = 1, 2 \cdots N$) sub-beam can be expressed as

$$\begin{bmatrix} \boldsymbol{C}^{w}_{n+1} \\ \boldsymbol{C}^{v}_{n+1} \end{bmatrix} = \left(\prod_{i=1}^{n} \mathbf{H}_{n-i+1}\right)\hat{\mathbf{H}}_1 \begin{bmatrix} \boldsymbol{C}^{w}_{1} \\ \boldsymbol{C}^{v}_{1} \end{bmatrix} + \left(\prod_{i=1}^{n} \hat{\mathbf{H}}_{n-i+1}\right)\mathbf{H}_F\hat{\boldsymbol{F}} \tag{59}$$

Case 2. *m* = *2, 3* $\cdots$ *N*

Similarly, the relationship between the integration constants of the $N+1$th and the 1th sub-beam can be expressed as

$$\begin{bmatrix} \boldsymbol{C}_{N+1}^{w} \\ \boldsymbol{C}_{N+1}^{v} \end{bmatrix} = \left(\prod_{i=1}^{N-m+1} \mathbf{H}_{N-i+1} \right) \hat{\mathbf{H}}_m \left(\prod_{i=N-m+2}^{N} \mathbf{H}_{N-i+1} \right) \begin{bmatrix} \boldsymbol{C}_1^{w} \\ \boldsymbol{C}_1^{v} \end{bmatrix} + \left(\prod_{i=1}^{N-m+1} \mathbf{H}_{N-i+1} \right) \mathbf{H}_F \hat{\boldsymbol{F}} \tag{60}$$

Then, the boundary conditions can be expressed as

$$\underbrace{\begin{bmatrix} \mathbf{B}_{\mathrm{L}\,6\times12} \\ \mathbf{B}_{\mathrm{R}\,6\times12} \left(\prod_{i=1}^{N-m+1} \mathbf{H}_{N-i+1} \right) \hat{\mathbf{H}}_m \left(\prod_{i=N-m+2}^{N} \mathbf{H}_{N-i+1} \right) \end{bmatrix}}_{12\times12} \begin{bmatrix} \boldsymbol{C}_1^{w} \\ \boldsymbol{C}_1^{v} \end{bmatrix} = \underbrace{\begin{bmatrix} 0_{6\times1} \\ -\mathbf{B}_{\mathrm{R}\,6\times12} \left(\prod_{i=1}^{N-m+1} \mathbf{H}_{N-i+1} \right) \mathbf{H}_F \hat{\boldsymbol{F}} \end{bmatrix}}_{12\times1} = \overline{\boldsymbol{F}} \tag{61}$$

Next, substituting Equation (61) into Equation (60), the integration constant parameters for the first component can be obtained:

$$\begin{bmatrix} \boldsymbol{C}_1^{w} \\ \boldsymbol{C}_1^{v} \end{bmatrix} = \begin{bmatrix} \mathbf{B}_{\mathrm{L}\,6\times12} \\ \mathbf{B}_{\mathrm{R}\,6\times12} \left(\prod_{i=1}^{N-m+1} \mathbf{H}_{N-i+1} \right) \hat{\mathbf{H}}_m \left(\prod_{i=N-m+2}^{N} \mathbf{H}_{N-i+1} \right) \end{bmatrix}^{-1} \overline{\boldsymbol{F}} \tag{62}$$

Introducing Equation (62) into Equation (60) leads to the integration constants of the n + 1 (n = 1, 2· · · N) sub-beam:

$$\begin{bmatrix} \boldsymbol{C}_{n+1}^{w} \\ \boldsymbol{C}_{n+1}^{v} \end{bmatrix} = \begin{cases} \left(\prod_{i=1}^{n} \mathbf{H}_{n-i+1} \right) \begin{bmatrix} \boldsymbol{C}_1^{w} \\ \boldsymbol{C}_1^{v} \end{bmatrix} & n = 1, 2 \cdots m-1 \\ \left\{ \left(\prod_{i=1}^{n-m+1} \mathbf{H}_{n-i+1} \right) \hat{\mathbf{H}}_m \left(\prod_{i=n-m+2}^{n} \mathbf{H}_{n-i+1} \right) \begin{bmatrix} \boldsymbol{C}_1^{w} \\ \boldsymbol{C}_1^{v} \end{bmatrix} + \left(\prod_{i=1}^{n-m+1} \mathbf{H}_{n-i+1} \right) \mathbf{H}_F \hat{\boldsymbol{F}} \right\} & n = m, 2 \cdots N \end{cases} \tag{63}$$

Case 3. *m* = *N* + *1*

For the similar derivations, the expressions of these constants are

$$\begin{bmatrix} \boldsymbol{C}_{n+1}^{w} \\ \boldsymbol{C}_{n+1}^{v} \end{bmatrix} = \left\{ \left(\prod_{i=1}^{n} \mathbf{H}_{n-i+1} \right) \begin{bmatrix} \boldsymbol{C}_1^{w} \\ \boldsymbol{C}_1^{v} \end{bmatrix} \quad n = 1, 2 \cdots N \right. \tag{64}$$

where

$$\begin{bmatrix} \boldsymbol{C}_1^{w} \\ \boldsymbol{C}_1^{v} \end{bmatrix} = \begin{bmatrix} \mathbf{B}_{\mathrm{L}\,6\times12} \\ \mathbf{B}_{\mathrm{R}\,6\times12} \hat{\mathbf{H}}_{N+1} \left(\prod_{i=1}^{N} \mathbf{H}_{N-i+1} \right) \end{bmatrix}^{-1} \overline{\boldsymbol{F}} \tag{65}$$

with

$$\overline{\boldsymbol{F}} = \underbrace{\begin{bmatrix} 0_{6\times1} \\ \mathbf{B}_{\mathrm{R}\,6\times12} \mathbf{H}_F \hat{\boldsymbol{F}} \end{bmatrix}}_{12\times1} \tag{66}$$

2.2.3. Force Excitation at the Subsystem

If the excitation force is applied at the mth subsystem, the compatibility conditions across the spring connection point can be expressed as

$$\mathbf{T}_{Rm}^{w} \boldsymbol{C}_{m+1}^{w} = \mathbf{T}_{Lm}^{w} \boldsymbol{C}_{m}^{w} + \boldsymbol{F}\boldsymbol{e}^{w} \tag{67}$$

$$\mathbf{T}_{Ri}^{\psi} \boldsymbol{C}_{m+1}^{w} = \mathbf{T}_{Lm}^{\psi} \boldsymbol{C}_{m}^{w} + \mathbf{T}_{Lm}^{\psi v} \boldsymbol{C}_{m}^{v} + \boldsymbol{T}\boldsymbol{e}^{\psi} \tag{68}$$

$$\mathbf{T}_{Rm}^{v} \boldsymbol{C}_{m+1}^{v} = \mathbf{T}_{Lm}^{v} \boldsymbol{C}_{m}^{v} + \mathbf{T}_{Lm}^{v\psi} \boldsymbol{C}_{m}^{\psi} + \boldsymbol{F}\boldsymbol{e}^{v} \tag{69}$$

where $\boldsymbol{Fe}^{w}$= $[0\ 0\ 0\ Fe^{w}]^T$, $\boldsymbol{Te}^{\psi}$= $[0\ 0\ 0\ Te^{\psi}]^T$, $\boldsymbol{Fe}^{v}$= $[0\ 0\ 0\ Fe^{v}]^T$.

Combining Equations (67)–(69) and organizing them in matrix form, one obtains:

$$\underbrace{\begin{bmatrix} \mathbf{T}_{Rm}^{w} & 0_{4\times4} \\ \mathbf{T}_{Rm}^{\psi} & 0_{4\times4} \\ 0_{4\times8} & \mathbf{T}_{Rm}^{v} \end{bmatrix}}_{12\times12} \underbrace{\begin{bmatrix} \boldsymbol{C}_{m+1}^{w} \\ \boldsymbol{C}_{m+1}^{v} \end{bmatrix}}_{8\times1} = \underbrace{\begin{bmatrix} \mathbf{T}_{Lm}^{w} & 0_{4\times4} \\ \mathbf{T}_{Lm}^{\psi} & \mathbf{T}_{Lm}^{\psi v} \\ \mathbf{T}_{Lm}^{v\psi} & \mathbf{T}_{Lm}^{v} \end{bmatrix}}_{12\times12} \underbrace{\begin{bmatrix} \boldsymbol{C}_{m}^{w} \\ \boldsymbol{C}_{m}^{v} \end{bmatrix}}_{8\times1} + \underbrace{\begin{bmatrix} \boldsymbol{Fe}^{w} \\ \boldsymbol{Te}^{\psi} \\ \boldsymbol{Fe}^{v} \end{bmatrix}}_{12\times1} \tag{70}$$

Then, the transitive relationship between the integration constants of the *i*th and the *i* + 1th sub-beam is

$$\begin{bmatrix} \boldsymbol{C}_{m+1}^{w} \\ \boldsymbol{C}_{m+1}^{v} \end{bmatrix} = \begin{bmatrix} \mathbf{T}_{Rm}^{w} & 0_{4\times4} \\ \mathbf{T}_{Rm}^{\psi} & 0_{4\times4} \\ 0_{4\times8} & \mathbf{T}_{Rm}^{v} \end{bmatrix}^{-1} \begin{bmatrix} \mathbf{T}_{Lm}^{w} & 0_{4\times4} \\ \mathbf{T}_{Lm}^{\psi} & \mathbf{T}_{Lm}^{\psi v} \\ \mathbf{T}_{Lm}^{v\psi} & \mathbf{T}_{Lm}^{v} \end{bmatrix} \begin{bmatrix} \boldsymbol{C}_{m}^{w} \\ \boldsymbol{C}_{m}^{v} \end{bmatrix} + \begin{bmatrix} \mathbf{T}_{Rm}^{w} & 0_{4\times4} \\ \mathbf{T}_{Rm}^{\psi} & 0_{4\times4} \\ 0_{4\times8} & \mathbf{T}_{Rm}^{v} \end{bmatrix}^{-1} \begin{bmatrix} \boldsymbol{Fe}^{w} \\ \boldsymbol{Te}^{\psi} \\ \boldsymbol{Fe}^{v} \end{bmatrix} = \mathbf{H}_m \begin{bmatrix} \boldsymbol{C}_{m}^{w} \\ \boldsymbol{C}_{m}^{v} \end{bmatrix} + \mathbf{H}_F \hat{\boldsymbol{Fe}} \tag{71}$$

By repeating Equation (71), the transitive relationship between the first sub-beam and the last sub-beam can be written as

$$\begin{bmatrix} \boldsymbol{C}_{N+1}^{w} \\ \boldsymbol{C}_{N+1}^{v} \end{bmatrix} = \left(\prod_{i=1}^{N} \mathbf{H}_{N-i+1} \right) \begin{bmatrix} \boldsymbol{C}_{1}^{w} \\ \boldsymbol{C}_{1}^{v} \end{bmatrix} + \left(\prod_{i=1}^{N-m} \mathbf{H}_{N-i+1} \right) \hat{\boldsymbol{Fe}} \tag{72}$$

Next, the boundary conditions can be written as follows:

$$\underbrace{\begin{bmatrix} \mathbf{B}_{6\times12}^{\mathrm{L}} \\ \mathbf{B}_{6\times12}^{\mathrm{R}} \left(\prod\limits_{i=1}^{N} \mathbf{H}_{N-i+1} \right) \end{bmatrix}}_{12\times12} \boldsymbol{C}_1 = \begin{bmatrix} 0_{6\times1} \\ -\mathbf{B}_{6\times12}^{\mathrm{R}} \left(\prod\limits_{i=1}^{N-m} \mathbf{H}_{N-i+1} \right) \hat{\boldsymbol{Fe}} \end{bmatrix} = \overline{\boldsymbol{Fe}} \tag{73}$$

The substitution of Equation (73) into Equation (72) obtains the integration constants of the $n+1$ ($n = 1, 2 \cdots \mathrm{N}$) sub-beam:

$$\boldsymbol{C}_{n+1} = \begin{cases} \left(\prod\limits_{i=1}^{n} \mathbf{H}_{n-i+1} \right) \boldsymbol{C}_1 & n = 1 \ldots m-1 \\ \left(\prod\limits_{i=1}^{n} \mathbf{H}_{n-i+1} \right) \boldsymbol{C}_1 + \left(\prod\limits_{i=1}^{n-m} \mathbf{H}_{n-i+1} \right) \hat{\boldsymbol{Fe}} & n = m \ldots N \end{cases} \tag{74}$$

where $\boldsymbol{C}_1$ is the integration constants of the 1th sub-beam and

$$\boldsymbol{C}_1 = \begin{bmatrix} \mathbf{B}_{\mathrm{L}\,6\times12} \\ \mathbf{B}_{\mathrm{R}\,6\times12} \left(\prod\limits_{i=1}^{N} \mathbf{H}_{N-i+1} \right) \end{bmatrix}^{-1} \overline{\boldsymbol{Fe}} \tag{75}$$

From the derivations above, it is obvious that all of the computing matrices ($\mathbf{H}_i$, $\mathbf{B}_{\mathrm{L}}$, $\mathbf{B}_{\mathrm{R}}$ and $\mathbf{H}_F$) associated with $\boldsymbol{C}_i$ are not larger than 12×12, which will lead to a small-dimension matrix operation, and hence a significant computational advantage.

3. Validation of the Proposed Method

To validate the reliability of the proposed method, some of the results in this work are checked with those obtained from the conventional FEM. The motion equation of thin-walled beam system can be written as

$$[\mathbf{M}]\{\ddot{x}\} + [\mathbf{C}]\{\dot{x}\} + [\mathbf{K}]\{x\} = \{\boldsymbol{F}\} \tag{76}$$

where $[\mathbf{M}]$, $[\mathbf{K}]$ and $[\mathbf{C}]$ denote the mass, stiffness and damping matrix for the thin-walled beam system, $\{v\}$ represent the node displacement vector of beam, and $\{\boldsymbol{F}\}$ is the force vector. The overall matrixes are obtained by imposing the prescribed boundary condition and assembling the associated mass matrix [**Me**] stiffness matrix [**Ke**] and the damping matrix [**Ce**] of the constrained beam element, which are given in Appendix E.

Introducing harmonic solutions in the form

$$\{x\} = \{\overline{x}\}e^{i\Omega t} \tag{77}$$

The frequency response functions can be obtained as

$$\{\overline{x}\} = \left(-\Omega^2\mathbf{M} + i\Omega\mathbf{C} + \mathbf{K}\right)^{-1}\{F\} \tag{78}$$

The forced vibration of a elastically constraint thin-walled beam carrying three spring-damper-mass subsystem (See in Figure 4) is solved both by the presented method and conventional finite-element method. The geometrical and physical properties of the thin-walled beam system are given as: E = 2.1 × 10^{11} Pa, G = 80 × 10^{10} Pa, ρ = 7850 kg/m^3, I_z = 1.3745 × 10^{-4} m^4, I_y = 1.6625 × 10^{-4} m^4, J = 4.7657 × 10^5 m^4, Γ_0 = 2.2783 × 10^{-8} m^6, I_0 = 5.9992 × 10^{-4} m^4, A = 0.0116 m^2, L = 3 m, z_c = 0.0619 m, z_b = −0.0550 m, a = 0.26 m, b = 0.32 m, $K_z^L = K_z^R = K_y^L = K_y^R$ = 40,000 kN/m $C_z^L = C_z^R = C_y^L = C_y^R$ = 800 N·s/m, m_i = 100 kg, J_i = 53.33 kg·m^2, $K_{z,i}^L = K_{z,i}^R = K_{y,i}^L = K_{y,i}^R$ = 16,666.67 kN/m, $c_{z,i}^L = c_{z,i}^R = c_{y,i}^L = c_{y,i}^R$ = 33.33 N·s/m, l_1 = 0.8 m, l_2 = 0.8 m, l_3 = 0.8 m, l_4 = 0.8, l_1^L = 0.08 m, l_1^R = 0.36 m, l_2^L = 0.36 m, l_2^R = 0.08 m, l_3^L = 0.08 m, l_3^R = 0.36 m, i = 1,2,3.

Without loss of generality, the forced vibration of the thin-walled beam system with an excitation force ($F^w e^{i\Omega t}$, $F^\psi e^{i\Omega t}$, $F^v e^{i\Omega t}$) applied at P_1 (representing the end point of thin-walled beam), P_2 (representing the arbitrary position of the thin-walled beam) and P_3 (representing the subsystem) are calculated by the proposed method and FEM, respectively. The frequency responses of P_1, P_2, P_4, P_5 (right end of the beam) in each calculation are illustrated in Figure 5. It can be seen that the curves calculated by the proposed method are greatly consistent with FEM. Hence, it is believed that the analytical method and FEM are accurate and reliable.

The frequency responses of the bare beam at P_1, P_2, P_4, and P_5 with force applying at P_1 are illustrate in Figure 6. The comparison of Figures 5 and 6 reveals that the introduction of a subsystem can generate several anti-resonance bands, in which the three-DOF SDM systems act as absorbers for the thin-walled beams, leading to a high suppression of structural vibration transmission. Moreover, a special frequency bandwidth is observed, in which the magnitude of the frequency response at the excitation points is the largest and, the further the detection point deviates from the excitation points, the smaller the response is. This phenomenon indicates that the elastic vibration in the thin-walled beam is increasingly and dramatically decayed when moving from the right end to the left end. Therefore, this structure can be applied in engineering practice to restrain the vibration transmission in the thin-walled beam based on these results.

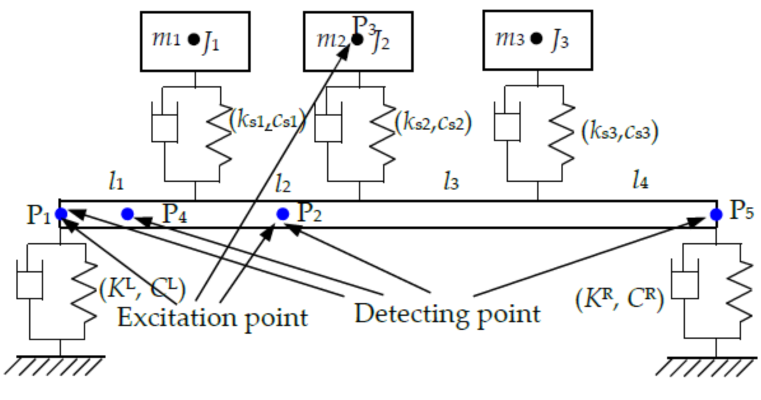

Figure 4. The front view of a thin-walled beam carrying three spring-damper-mass subsystems.

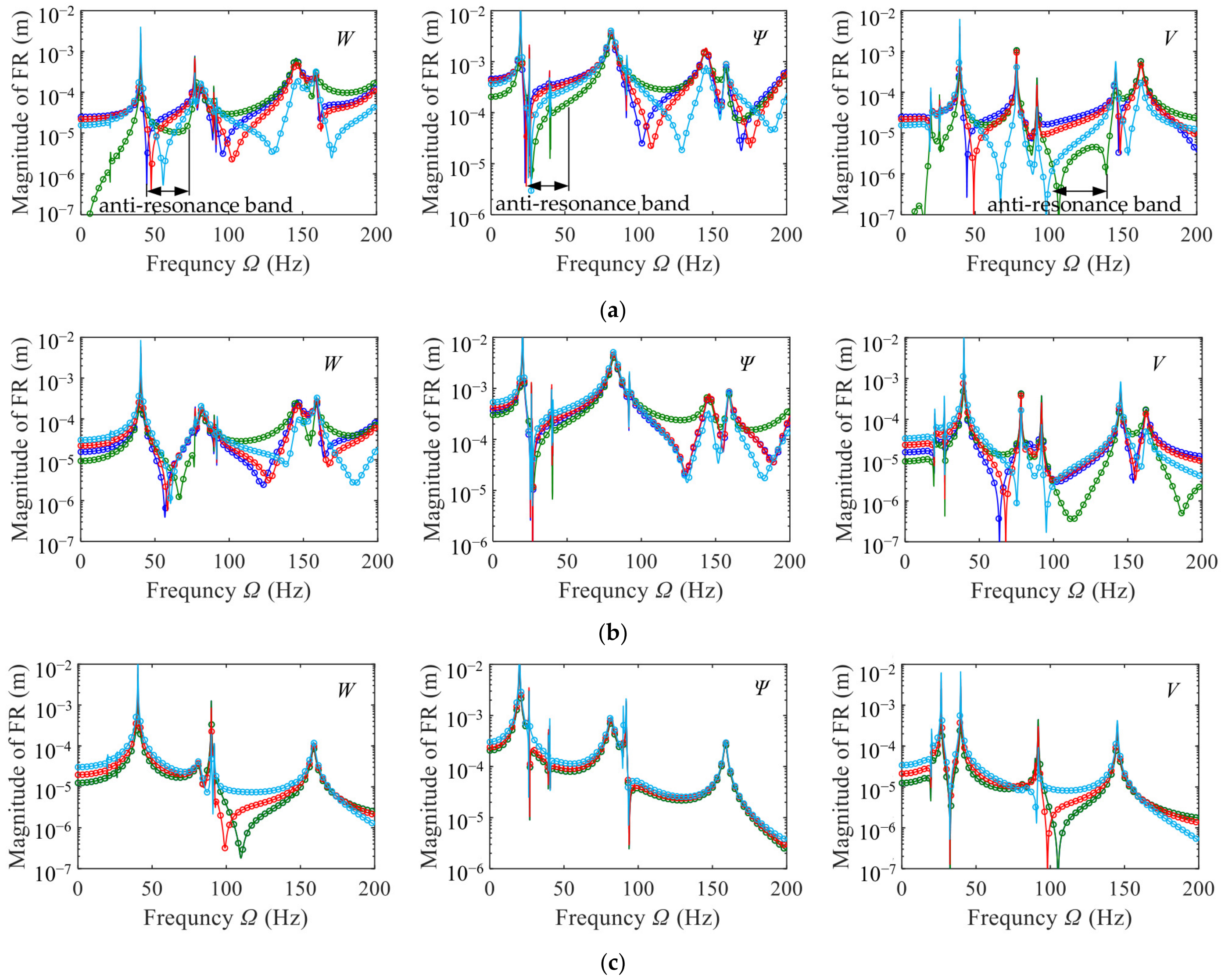

Figure 5. Frequency response at P_1, P_2, P_4, and P_5, as illustrated in Figure 4 (——— FR at P_1 with the presented method, ○ FR at P_1 with FEM, ——— FR at P_2 with the presented method, ○ FR at P_2 with FEM, ——— FR at P_4 with the presented method, ○ FR at P_4 with FEM, ——— FR at P_5 with the presented method, and ○ FR at P_5 with FEM). (**a**) Force is applied at P1; (**b**) Force is applied at P_2; (**c**) Force is applied at P_3.

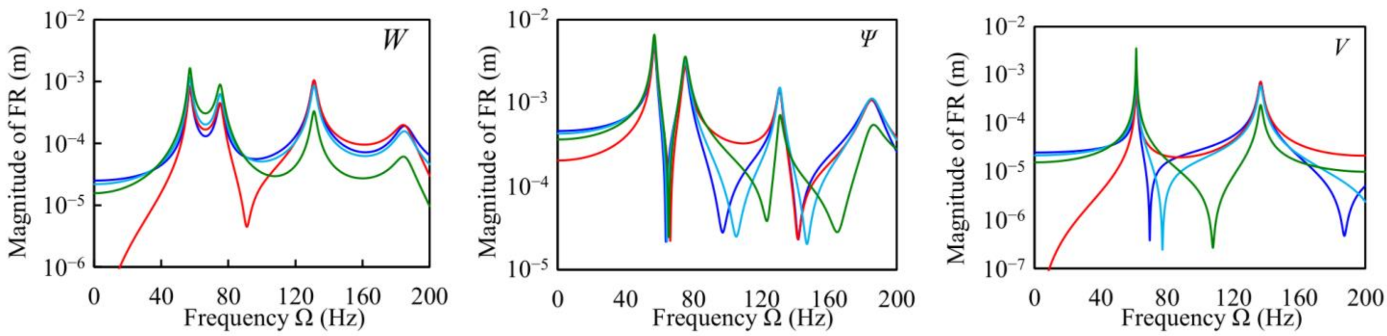

Figure 6. Frequency response of the bare beam at P_1, P_2, P_4, and P_5 with force applying at P_1. (——— FR at P_1, ——— FR at P_2, ——— FR at P_4, ——— FR at P_5).

4. Parameter Study and Discussion

4.1. Effect of Subsystem Parameters on Vibration Transmission of the Thin-Walled Beam

This subsection investigates the influence of the subsystem parameters on the frequency response (FR) at the right end of the beam. In this subsection, the stiffness and damping of the elastic constraints are set to 0, and the excitation force ($F^w e^{i\Omega t}$, $F^\psi e^{i\Omega t}$, $F^v e^{i\Omega t}$) is applied at the left end of the beam.

Figure 7 illustrates the Frequency Response at the right end of the beam with symmetrical $l_i^{\mathrm{L}} = l_i^{\mathrm{L}} = 0.22$ m) and asymmetric ($l_1^{\mathrm{L}} = 0.08$ m, $l_1^{\mathrm{R}} = 0.36$ m, $l_2^{\mathrm{L}} = 0.36$ m, $l_2^{\mathrm{R}} = 0.08$ m, $l_3^{\mathrm{L}} = 0.08$ m, $l_3^{\mathrm{R}} = 0.36$ m) subsystems. The introduction of asymmetric subsystems is able to make the bending vibration in W direction and the torsional vibration of the thin-walled beam couple with the bending vibration of it in V direction, which are independent in the thin-walled beam with symmetrical subsystems. The vibration of subsystem in z direction and θ direction will couple strongly when the centroidal deviation of subsystem is large, which leads to all the degrees of freedom of the whole system coupling with each other. Notice that (1) when the excitation force is applied in W direction, the force transmission path is W-y, W-Ψ-θ-z-V; (2) when the excitation force is applied in Ψ direction, the force transmission path is Ψ-W-y, Ψ-θ-z-V; (3) when the excitation force is applied in V direction, the force transmission path is V-z-θ-Ψ-W-y. Moreover, the vibration coupling is very strong at low frequencies ($\Omega < 2200$ Hz) since the natural frequencies of low order modes of the thin-walled are close to the natural frequencies of subsystems; thus, the bending vibration in W directions and the torsional vibration of the thin-walled beam strongly couple with the bending vibration of it in V direction via the force transmission of subsystem; conversely, the natural frequencies of high order modes are much higher than the subsystems, which result in a very slight force transmission between the three directions of thin-walled beam, and lead to a significant weak vibration coupling between them.

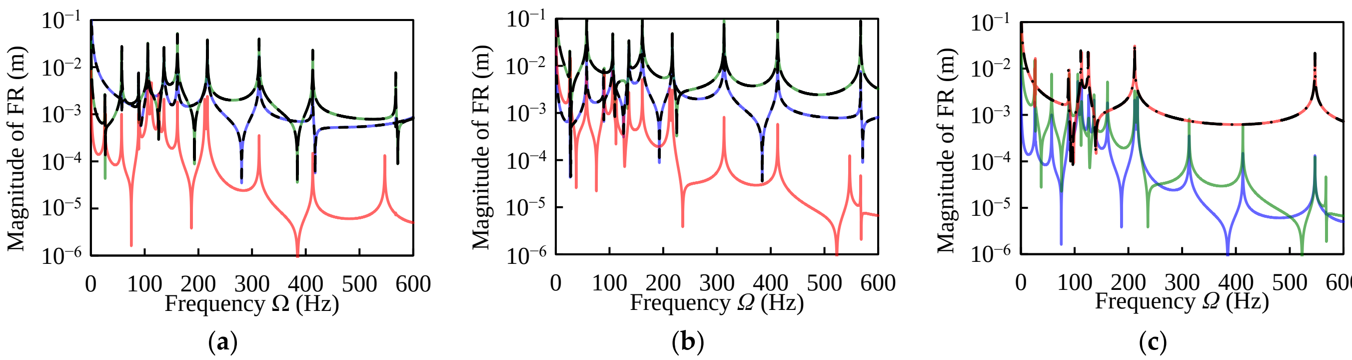

Figure 7. FR at the right end of the thin-walled beam with symmetrical and asymmetrical subsystems. (——— W (with symmetrical systems), – – – – W (with asymmetrical systems), ——— Ψ (with symmetrical systems) - - - - - - Ψ (with asymmetrical systems) ——— V (with symmetrical systems), – · – · – V (with asymmetrical systems)). (**a**) Force is applied in W direction; (**b**) Force is applied in Ψ direction; (**c**) Force is applied in V direction.

The effects of the subsystems' stiffness k_{si}, damping c_{si}, mass m_i, moment of inertia J_i on the vibration transmission characteristics of the thin-walled beam are illustrated in Figures 8 and 9, respectively. Figure 8 shows that the location of the anti-resonance bands can be adjusted by the subsystems' stiffness to suppress the vibration with a specific frequency, since their move to a higher frequency area with the increase of k_{si}. Figure 9 reveals that a larger damping of the subsystem is helpful for the suppression of vibration transmission in the thin-walled beams, since c_{si} can significantly decrease the peak values of FR. It can be observed in Figure 10 that, when the mass is small, the resonance peaks and anti-resonance points generated by the subsystems are very weak, since the translational motion mode of subsystems (J_i is relatively small) are not strong enough to affect the vibration characteristic of the whole system; by increasing the value of m_i, the effect of subsystems on vibration characteristic of the whole thin-walled system become stronger, resulting in more remarkable resonance peaks and anti-resonance points. It is worth noting that a higher m_i corresponds to a decrease in the frequency of the potential well in Ψ direction, accompanying an increase in the width of the frequency band. Figure 11 shows the moment of inertia of the subsystem has a great effect on the vibration transmission potential well in all three directions. Generally, a higher J_i corresponds to a decrease in the frequency of the anti-resonance band.

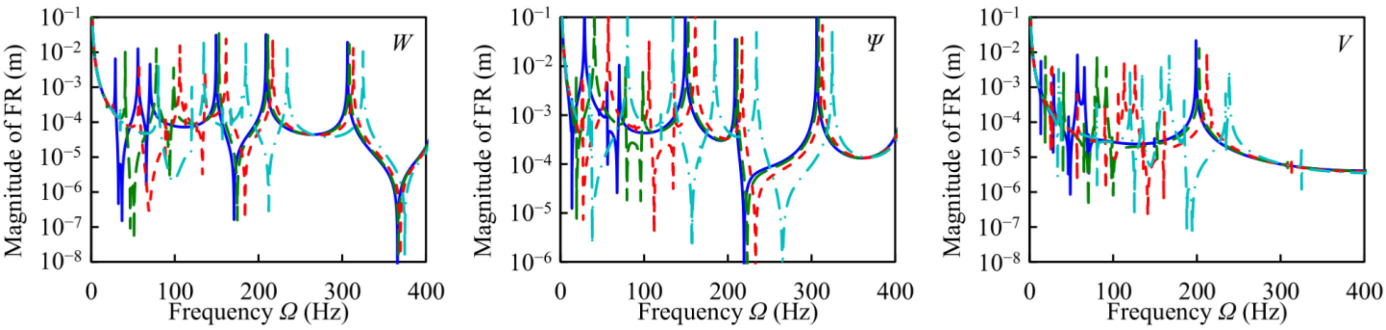

Figure 8. Effect of the stiffness of the subsystem on the frequency response at the right end of the thin-walled beam (k_{si} = 3333.33/2 kN/m, k_{si} = 3333.33 kN/m, k_{si} = 3333.33 × 2 kN/m, k_{si} =3333.33 × 4 kN/m).

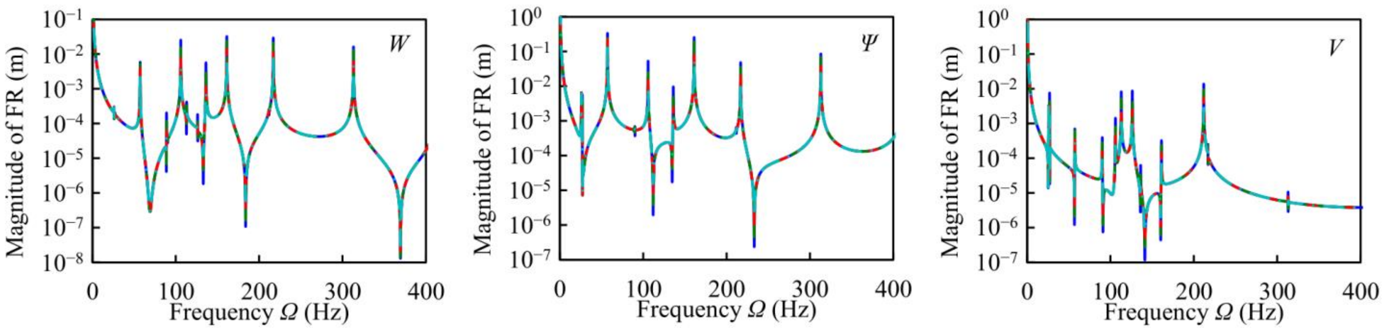

Figure 9. Effect of the damping of the subsystem on the frequency response at the right end of the beam (c_{si} = 66.67/2 N·s/m, c_{si} =66.67 N·s/m, c_{si} =66.67 × 2 N·s/m, c_{si} = 66.67 × 4 N·s/m).

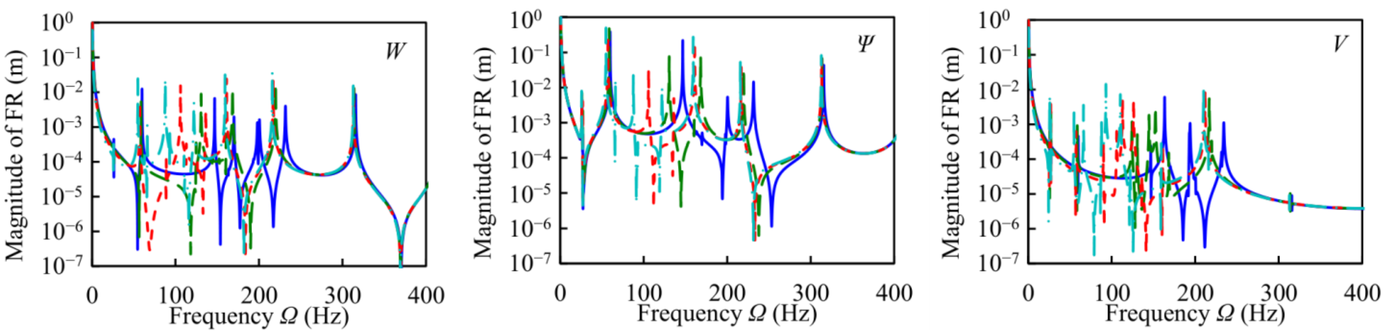

Figure 10. Effect of the mass of the subsystem on the frequency response at the right end of the beam (m_i = 266.67/2 kg, m_i = 266.67 kg, m_i = 266.67 × 2 kg, m_i = 266.67 × 4 kg).

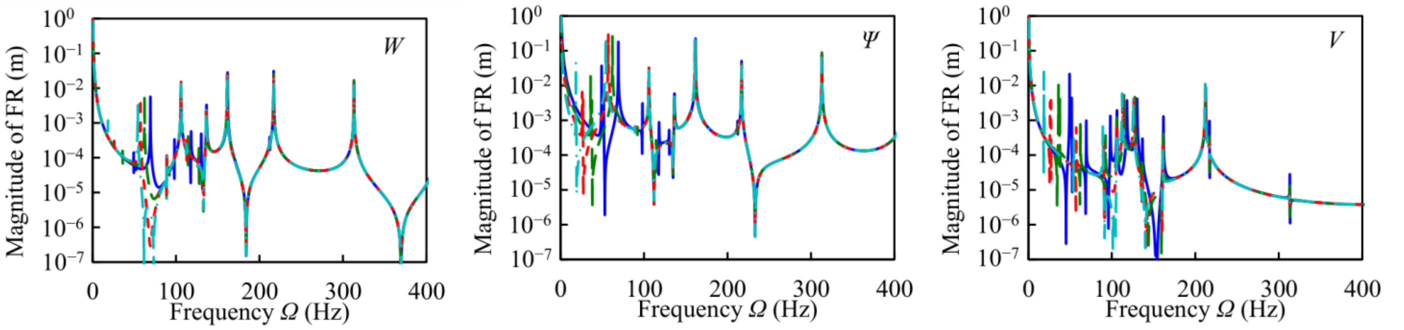

Figure 11. Effect of the moment of inertia of the subsystem on the frequency response at the right end of the beam (——— J_i = 53.33/2 kg·m^2, – – – – J_i = 53.33 kg·m^2, – · – · – J_i = 53.33 × 2 kg·m^2, --------- Ji = 53.33 × 4 kg·m^2).

Apparently, a relatively deeper and wider anti-resonance band can guarantee effective restraint of the vibration transmission in the beam, hence the parameter design of the subsystem should follow the following principle: (1) For an excitation force with a relatively high frequency, the stiffness of subsystem should be large; (2) For an excitation force with a relatively low frequency, larger mass and moment of inertia are required.

4.2. Effect of Parameters on the Vibration Isolation Characteristic of the Thin-Walled Beams Systems

For the system, consisting of power machines and thin-walled structures, the isolation of the excitation force of the machines' transfer to the structures is a main measure to control the structure vibration and noise radiation of the system. Obviously, the parameters of the elastic suspensions and the position of the machines are believed to significantly influence the dynamic response of the thin-walled beam. This subsection studies the relationship between these parameters and the dynamic response of the thin-walled beam. The system is illustrated in Figure 12, and the parameters of the system were arbitrarily selected as follows: $K_z^L = K_z^R = K_y^L = K_y^R$ = 40,000 kN/m, $C_z^L = C_z^R = C_y^L = C_y^R$ = 800 N·s/m, $K_T^L = K_T^R$ = 1500 kN·m/rad; $K_T^L = K_T^R$ = 300 N·m·s/rad; m = 300 kg, J = 160 kg·m^2, $k_z^L = k_z^R = k_y^L = k_y^R = k_s$ = 40,000 kN/m, $c_z^L = c_z^R = c_y^L = c_y^R$ = 100 N·s/m, l_1 = 1.6 m, l_2 = 1.6 m, l_1^L = 0.08 m, l_1^R = 0.36 m.

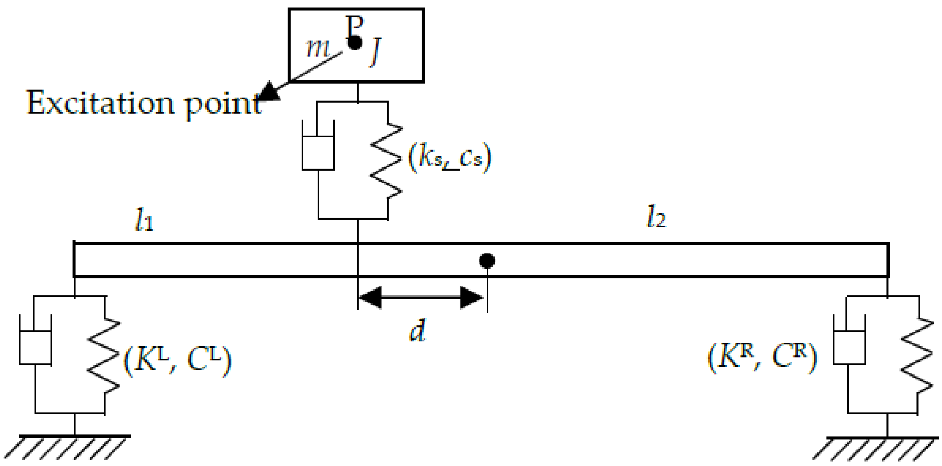

Figure 12. The front view of an elastically constrained thin-beam carrying a spring-damper-mass subsystem.

In order to accurately describe the intensity of the structural vibration, the vibration energy of the thin-walled beam is defined as follows:

$$EV = EK/\Omega^2 = \int \rho A(W(x)^2 + V(x)^2) + \rho I_0 \Psi(x)^2 dx \tag{79}$$

where EK is the kinetic energy of the thin-walled beam.

The influences of the subsystems' stiffness k_{si}, damping c_{si}, location d (the distance between the subsystem and the symmetry center of the thin-walled beam), elastic constraint stiffness K and elastic constraint damping C on the vibration isolation characteristics of the thin-walled beam systems are illustrated in Figures 13–17, respectively. It can be observed for Figure 13 that the high frequency magnitude of EV increases with the increase in k_{si} due to the increasing coupling degree of the rigid motion of the subsystem and the higher order mode of the thin-walled beam. Figure 14 shows that a suitable lager c_{si} is helpful to suppress the resonance peaks values of EV, while the excessive damping will deteriorate the isolation performance of the thin-walled beam systems due to the bonding effect between the subsystem and beam. It can be seen from Figure 15 that the resonance peak values of EV decrease along with the increase of d, which also leads to an increased number of resonance peaks, since the stronger asymmetry of the system will cause more resonances mode. Figure 16 shows that the frequency of the resonance peaks increases with K due to the increase of the mode stiffness of the thin-walled beams. However, the excessive stiffness will decrease the mode damping coefficient of the thin-walled beam, resulting in a dramatic increase of the magnitude of the resonance peak of EV. Figure 17 reveals that the EV curves of the thin-walled for a higher C have a smaller peak value compared to that for a lower C due to the increase of the mode damping coefficient of the thin-walled beam.

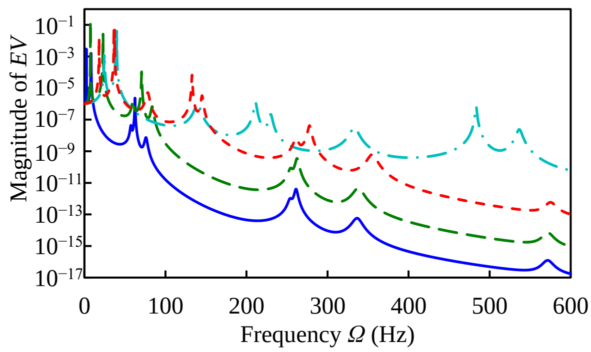

Figure 13. Effect of the stiffness of the subsystem on vibration energy of the thin-walled beam (——— k_s = 40,000/100 kN/m, — — — k_s = 40,000/10 kN/m, - - - - - k_s = 40,000 kN/m, — · — · — k_s = 40,000 × 10 kN/m).

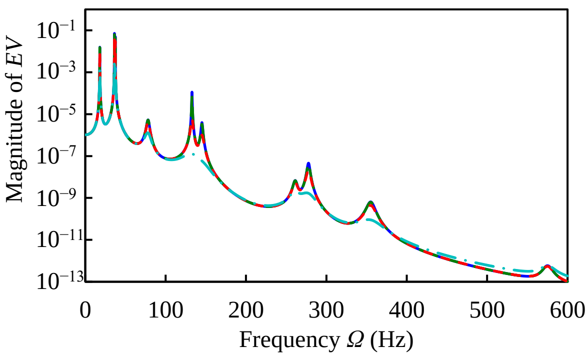

Figure 14. Effect of the damping of the subsystem on vibration energy of the thin-walled beam (——— c_s = 100/10 N·s/m, — — — c_s = 100 N·s/m kN/m, - - - - - c_s = 100 × 10 N·s/m, — · — · — k_s = 100 × 100 N·s/m).

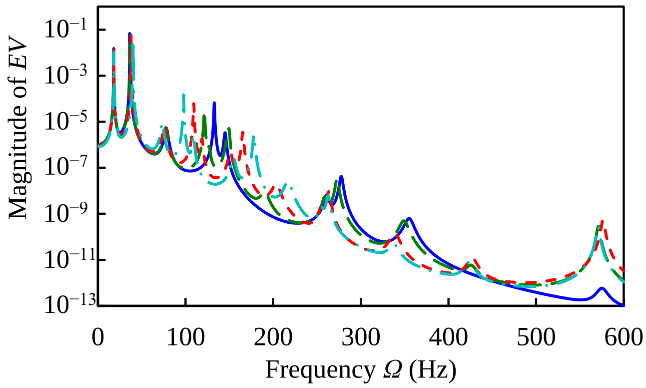

Figure 15. Effect of the distance between the machine and the beam's axis of symmetry on vibration energy of the thin-walled beam (——— d = 0 m, – – – – d = 0.3 m, - - - - - - d = 0.6 m, – · – · – d = 0.9 m).

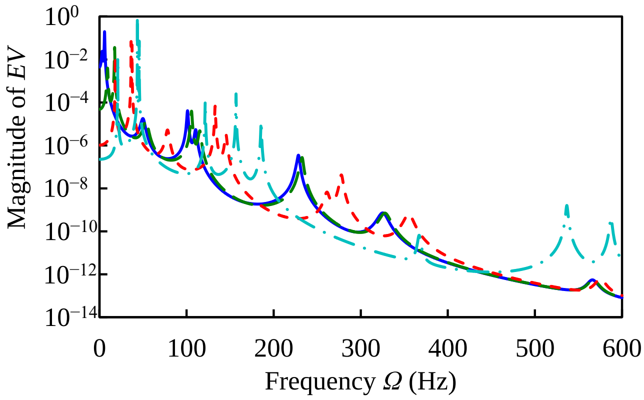

Figure 16. Effect of the stiffness of elastic constraint on vibration energy of the thin-walled beam (——— K/100, – – – – K/10, - - - - - - K, – · – · – K×10, K = (K_y, K_z, K_T)).

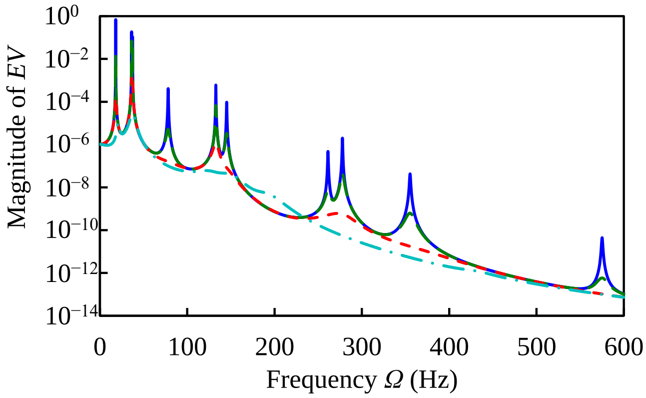

Figure 17. Effect of the damping of the elastic constraint on vibration energy of the thin-walled beam (——— C/10, – – – – C, - - - - - - C × 10, – · – · – C × 100, C= (C_y, C_z, C_T)).

Based on the above discussions, relatively smaller stiffnesses and larger damping of the subsystem and elastic constraint are beneficial to isolate the excitation force of the machines from the base structures.

5. Conclusions

This paper presents a new closed analytical approach to obtaining the forced vibration of bending-torsional-warping coupled thin-walled beams with an arbitrary number of 3-DoF spring-damper-mass subsystems and boundary conditions based on the transfer matrix approach and dynamic condensation methods. The thin-walled beam is divided into a series of distinct sub-beams whose ends are connected to the SDM subsystems. The transfer matrix for each sub-beam is developed based on the exact shape functions of the bending-torsional-warping coupling Euler-Bernoulli theory. Each SDM system is modeled by a set of effective springs based on the dynamic condensation method. The governing matrix equation is formulated based on the compatibility conditions of the placement and the force at the common interfaces of two adjacent sub-beams.

The proposed method is very convenient to apply and can be conveniently used to obtain exact close form expression of the frequency response function; it enables simultaneous consideration of arbitrary boundary conditions and an arbitrary number of SDM systems; furthermore, the proposed method reasonably yields the associate matrixes with size never larger than 12 × 12 independent of the number of subsystems, thus leading to a significant computational advantage.

The results computed by the proposed method achieve good agreement with those obtained by the conventional finite-element method. The effects of the system parameters on the vibration transmission and vibration isolation properties of the thin-walled beam system are studied. The results provide useful information for the analysis and design of thin-walled structures with power machines for the purposes of elastic vibration transmission reduction and vibration isolation.

Author Contributions: Conceptualization, X.L. and J.C.; methodology, X.L. and J.C.; software, J.C.; validation, X.L. and J.C.; formal analysis, J.C.; investigation, J.C.; resources, J.C.; data curation, J.C.; writing—original draft preparation, J.C.; writing—review and editing, X.L. and J.C.; visualization, J.C.; supervision, X.L. and J.C.; project administration, J.C.; funding acquisition, J.C. All authors have read and agreed to the published version of the manuscript.

Funding: This research was funded by the Natural science foundation of Hunan Province grant number 2022JJ40592 and science and technology innovation Program of Hunan Province grant number 2021RC2009.

Conflicts of Interest: The authors declare no conflict of interest.

Appendix A

The Derivations of Equations (1)–(10)

If the external loads on the three-DOF SDM system is zero, then from Figure 2a one obtains

$$F_{z,i}^{\mathrm{L}} = k_{z,i}^{\mathrm{L}}(u_{z,i}^{\mathrm{L}} - v_{z,i}^{\mathrm{L}}) + c_{z,i}^{\mathrm{L}}(\dot{u}_{z,i}^{\mathrm{L}} - \dot{v}_{z,i}^{\mathrm{L}}) \;\; F_{z,i}^{\mathrm{R}} = k_{z,i}^{\mathrm{R}}(u_{z,i}^{\mathrm{R}} - v_{z,i}^{\mathrm{R}}) + c_{z,i}^{\mathrm{R}}(\dot{u}_{z,i}^{\mathrm{R}} - \dot{v}_{z,i}^{\mathrm{R}}) \tag{A1}$$

$$F_{y,i}^{\mathrm{L}} = k_{y,i}^{\mathrm{L}}(u_{y,i}^{\mathrm{L}} - v_{y,i}^{\mathrm{L}}) + c_{y,i}^{\mathrm{L}}(\dot{u}_{y,i}^{\mathrm{L}} - \dot{v}_{y,i}^{\mathrm{L}}) \;\; F_{y,i}^{\mathrm{R}} = k_{y,i}^{\mathrm{R}}(u_{y,i}^{\mathrm{R}} - v_{y,i}^{\mathrm{R}}) + c_{y,i}^{\mathrm{R}}(\dot{u}_{y,i}^{\mathrm{R}} - \dot{v}_{y,i}^{\mathrm{R}}) \tag{A2}$$

where $F_{z,i}^{\mathrm{L}}$, $F_{z,i}^{\mathrm{R}}$, $F_{y,i}^{\mathrm{L}}$ and $F_{y,i}^{\mathrm{R}}$ are, respectively, the internal force of springs $k_{z,i}^{\mathrm{L}}$, $k_{z,i}^{\mathrm{R}}$, $k_{y,i}^{\mathrm{L}}$ and $k_{y,i}^{\mathrm{R}}$, and $u_{z,i}^{\mathrm{L}} = z_i - l_i^{\mathrm{L}}\theta_i$, $u_{z,i}^{\mathrm{R}} = z_i + l_i^{\mathrm{R}}\theta_i$, $u_{y,i}^{\mathrm{L}} = u_{y,i}^{\mathrm{R}} = y_i$.

According to Newton's second law, the dynamic equation of the two-DOF SDM system can be written as

$$m_i\ddot{y}_i + F_{y,i}^{\mathrm{L}} + F_{y,i}^{\mathrm{R}} = 0 \tag{A3}$$

$$m_i\ddot{z}_i + F_{z,i}^{\mathrm{L}} + F_{z,i}^{\mathrm{R}} = 0 \tag{A4}$$

$$J_i\ddot{\theta}_i - F_{z,i}^{\mathrm{L}} l_i^{\mathrm{L}} + F_{z,i}^{\mathrm{R}} l_i^{\mathrm{L}} = 0 \tag{A5}$$

Substituting Equations (A1) and (A2) into Equations (A3)–(A5) yields

$$m_i\ddot{y}_i + k_{y,i}^{\mathrm{L}}(y_i - v_{y,i}^{\mathrm{L}}) + c_{y,i}^{\mathrm{L}}(\dot{y}_i - \dot{v}_{y,i}^{\mathrm{L}}) + k_{y,i}^{\mathrm{R}}(y_i - v_{y,i}^{\mathrm{R}}) + c_{y,i}^{\mathrm{R}}(\dot{y}_i - \dot{v}_{y,i}^{\mathrm{R}}) = 0 \tag{A6}$$

$$m_i\ddot{z}_i + k_{z,i}^{\mathrm{L}}(z_i - l_i^{\mathrm{L}}\theta_i - v_{z,i}^{\mathrm{L}}) + c_{z,i}^{\mathrm{L}}(\dot{z}_i - l_i^{\mathrm{L}}\dot{\theta}_i - \dot{v}_{z,i}^{\mathrm{L}}) + k_{z,i}^{\mathrm{R}}(z_i + l_i^{\mathrm{R}}\theta_i - v_{z,i}^{\mathrm{R}}) + c_{z,i}^{\mathrm{R}}(\dot{z}_i + l_i^{\mathrm{R}}\dot{\theta}_i - \dot{v}_{z,i}^{\mathrm{R}}) = 0 \tag{A7}$$

$$J_i\ddot{\theta}_i - k_{z,i}^{\mathrm{L}} l_i^{\mathrm{L}}(z_i - l_i^{\mathrm{L}}\theta_i - v_{z,i}^{\mathrm{L}}) - c_{z,i}^{\mathrm{L}} l_i^{\mathrm{L}}(\dot{z}_i - l_i^{\mathrm{L}}\dot{\theta}_i - \dot{v}_{z,i}^{\mathrm{L}}) + k_{z,i}^{\mathrm{R}} l_i^{\mathrm{R}}(z_i + l_i^{\mathrm{R}}\theta_i - v_{z,i}^{\mathrm{R}}) + c_{z,i}^{\mathrm{R}} l_i^{\mathrm{R}}(\dot{z}_i + l_i^{\mathrm{R}}\dot{\theta}_i - \dot{v}_{z,i}^{\mathrm{R}}) = 0 \tag{A8}$$

For the damped force vibration of the loading beam (beam with lumped mass system), one has

$$\begin{array}{l} u_{y,i}^{\mathrm{L}} = \overline{u}_{y,i}^{\mathrm{L}} e^{\overline{\omega} t} \; u_{y,i}^{\mathrm{R}} = \overline{u}_{y,i}^{\mathrm{R}} e^{\overline{\omega} t} \; u_{z,i}^{\mathrm{L}} = \overline{u}_{z,i}^{\mathrm{L}} e^{\overline{\omega} t} \; u_{z,i}^{\mathrm{R}} = \overline{u}_{z,i}^{\mathrm{R}} e^{\overline{\omega} t} \; v_{y,i}^{\mathrm{L}} = \overline{v}_{y,i}^{\mathrm{L}} e^{\overline{\omega} t} \; v_{y,i}^{\mathrm{R}} = \overline{v}_{y,i}^{\mathrm{R}} e^{\overline{\omega} t} \\ v_{z,i}^{\mathrm{L}} = \overline{v}_{z,i}^{\mathrm{L}} e^{\overline{\omega} t} \; v_{z,i}^{\mathrm{R}} = \overline{v}_{z,i}^{\mathrm{R}} e^{\overline{\omega} t} \; y_i = \overline{y}_i e^{\overline{\omega} t} \; z_i = \overline{z}_i e^{\overline{\omega} t} \; \theta_i = \overline{\theta}_i e^{\overline{\omega} t} \end{array} \tag{A9}$$

where $\overline{\omega} = \Omega\ \bar{i}$, Ω is the frequency of the excitation force; t is time and $\bar{i} = \sqrt{-1}$.

Introducing Equation (A9) into Equations (A6)–(A8), then writing the results in matrix form, one obtains

$$y_i = \frac{(\overline{\omega} c_{y,i}^{\mathrm{L}} + k_{y,i}^{\mathrm{L}})}{m_i \overline{\omega}^2 + \overline{\omega}(c_{y,i}^{\mathrm{L}} + c_{y,i}^{\mathrm{R}}) + (k_{y,i}^{\mathrm{L}} + k_{y,i}^{\mathrm{R}})} v_{y,i}^{\mathrm{L}} + \frac{(\overline{\omega} c_{y,i}^{\mathrm{R}} + k_{y,i}^{\mathrm{R}})}{m_i \overline{\omega}^2 + \overline{\omega}(c_{y,i}^{\mathrm{L}} + c_{y,i}^{\mathrm{R}}) + (k_{y,i}^{\mathrm{L}} + k_{y,i}^{\mathrm{R}})} v_{y,i}^{\mathrm{R}} \tag{A10}$$

$$\begin{array}{l} \left\{ \begin{array}{c} z_i \\ \theta_i \end{array} \right\} = \left[\begin{array}{cc} m_i \overline{\omega}^2 + \overline{\omega}(c_{z,i}^{\mathrm{L}} + c_{z,i}^{\mathrm{R}}) + (k_{z,i}^{\mathrm{L}} + k_{z,i}^{\mathrm{R}}) & -(k_{z,i}^{\mathrm{L}} l_i^{\mathrm{L}} - k_{z,i}^{\mathrm{R}} l_i^{\mathrm{R}}) - \overline{\omega}(c_{z,i}^{\mathrm{L}} l_i^{\mathrm{L}} - c_{z,i}^{\mathrm{R}} l_i^{\mathrm{R}}) \\ -(k_{z,i}^{\mathrm{L}} l_i^{\mathrm{L}} - k_{z,i}^{\mathrm{R}} l_i^{\mathrm{R}}) - \overline{\omega}(c_{z,i}^{\mathrm{L}} l_i^{\mathrm{L}} - c_{z,i}^{\mathrm{R}} l_i^{\mathrm{R}}) & J_i \overline{\omega}^2 + \overline{\omega}(c_{z,i}^{\mathrm{L}} l_i^{\mathrm{L}\,2} + c_i^{\mathrm{R}} l_i^{\mathrm{R}\,2}) + (c_i^{\mathrm{L}} l_i^{\mathrm{L}\,2} + c_i^{\mathrm{R}} l_i^{\mathrm{R}\,2}) \end{array} \right]^{-1} \\ \times \left[\begin{array}{cc} k_{z,i}^{\mathrm{L}} + \overline{\omega} c_{z,i}^{\mathrm{L}} & k_{z,i}^{\mathrm{R}} + \overline{\omega} c_{z,i}^{\mathrm{R}} \\ -l_{z,i}^{\mathrm{L}}(k_{z,i}^{\mathrm{L}} + \overline{\omega} c_{z,i}^{\mathrm{L}}) & l_{z,i}^{\mathrm{R}}(k_{z,i}^{\mathrm{R}} + \overline{\omega} c_{z,i}^{\mathrm{R}}) \end{array} \right] \left\{ \begin{array}{c} v_{z,i}^{\mathrm{L}} \\ v_{z,i}^{\mathrm{R}} \end{array} \right\} \end{array} \tag{A11}$$

Substituting Equations (A9)–(A11) into Equations (A1) and (A2) leads to

$$F_{y,i}^{\mathrm{L}} = ke_{y,i}^{11} v_{y,i}^{\mathrm{L}} + ke_{y,i}^{12} v_{y,i}^{\mathrm{R}} \;\; F_{y,i}^{\mathrm{R}} = ke_{y,i}^{21} v_{y,i}^{\mathrm{L}} + ke_{y,i}^{22} v_{y,i}^{\mathrm{R}} \tag{A12}$$

$$F_{z,i}^{\mathrm{L}} = ke_{z,i}^{11} v_{z,i}^{\mathrm{L}} + ke_{z,i}^{12} v_{z,i}^{\mathrm{R}} \;\; F_{z,i}^{\mathrm{R}} = ke_{z,i}^{21} v_{z,i}^{\mathrm{L}} + ke_{z,i}^{22} v_{z,i}^{\mathrm{R}} \tag{A13}$$

where $k_{z,i}^{11}$, $k_{z,i}^{12}$, $k_{y,i}^{21}$, $k_{y,i}^{22}$ and $k_{z,i}^{11}$, $k_{z,i}^{12}$, $k_{y,i}^{21}$, $k_{y,i}^{22}$ are the stiffness of effective springs as shown in Figure 2b.

Appendix B

The Expression of Derivative Matrices in Equations (41)–(43) Are as Follows

$$\begin{array}{l} \mathbf{T}_{\mathrm{L}i}^{w} = \left[\begin{array}{cccc} \sinh\beta_1 l_i & \cosh\beta_1 l_i & \sinh\beta_2 l_i & \cosh\beta_2 l_i \\ \beta_1 \cosh\beta_1 l_i & \beta_1 \sinh\beta_1 l_i & \beta_2 \cosh\beta_2 l_i & \beta_2 \sinh\beta_2 l_i \\ {\beta_1}^2 \sinh\beta_1 l_i & {\beta_1}^2 \cosh\beta_1 l_i & {\beta_2}^2 \sinh\beta_2 l_i & {\beta_2}^2 \cosh\beta_2 l_i \\ t_i^{41} & t_i^{42} & t_i^{43} & t_i^{44} \end{array} \right. \\ \left. \begin{array}{cccc} \sinh\beta_3 l_i & \cosh\beta_3 l_i & \sinh\beta_4 l_i & \cosh\beta_4 l_i \\ \beta_3 \cosh\beta_3 l_i & \beta_3 \sinh\beta_3 l_i & \beta_4 \cosh\beta_4 l_i & \beta_4 \sinh\beta_4 l_i \\ {\beta_3}^2 \sinh\beta_3 l_i & {\beta_3}^2 \cosh\beta_3 l_i & {\beta_4}^2 \sinh\beta_4 l_i & {\beta_4}^2 \cosh\beta_4 l_i \\ t_i^{45} & t_i^{46} & t_i^{47} & t_i^{48} \end{array} \right] \end{array} \tag{A14}$$

$$\begin{array}{l} t_i^{41} = EI_y {\beta_1}^3 \cosh\beta_1 l_i + \overline{K} y_i \sinh\beta_1 l_i (1 + z_{\mathrm{b}} t_1),\; t_i^{42} = EI_y {\beta_1}^3 \sinh\beta_1 l_i + \overline{K} y_i \cosh\beta_1 l_i (1 + z_{\mathrm{b}} t_1) \\ t_i^{43} = EI_y {\beta_2}^3 \cosh\beta_2 l_i + \overline{K} y_i \sinh\beta_2 l_i (1 + z_{\mathrm{b}} t_2),\; t_i^{44} = EI_y {\beta_2}^3 \sinh\beta_2 l_i + \overline{K} y_i \cosh\beta_2 l_i (1 + z_{\mathrm{b}} t_2) \\ t_i^{45} = EI_y {\beta_3}^3 \cosh\beta_3 l_i + \overline{K} y_i \sinh\beta_3 l_i (1 + z_{\mathrm{b}} t_3),\; t_i^{46} = EI_y {\beta_3}^3 \sinh\beta_3 l_i + \overline{K} y_i \cosh\beta_3 l_i (1 + z_{\mathrm{b}} t_3) \\ t_i^{47} = EI_y {\beta_4}^3 \cosh\beta_4 l_i + \overline{K} y_i \sinh\beta_4 l_i (1 + z_{\mathrm{b}} t_4),\; t_i^{48} = EI_y {\beta_4}^3 \sinh\beta_4 l_i + \overline{K} y_i \cosh\beta_4 l_i (1 + z_{\mathrm{b}} t_4) \end{array}$$

$$\mathbf{T}_{\mathrm{R}i}^{w} = \left[\begin{array}{cccccccc} 0 & 1 & 0 & 1 & 0 & 1 & 0 & 1 \\ \beta_1 & 0 & \beta_2 & 0 & \beta_3 & 0 & \beta_4 & 0 \\ 0 & {\beta_1}^2 & 0 & {\beta_2}^2 & 0 & {\beta_3}^2 & 0 & {\beta_4}^2 \\ EI_y {\beta_1}^3 & 0 & EI_y {\beta_2}^3 & 0 & EI_y {\beta_3}^3 & 0 & EI_y {\beta_4}^3 & 0 \end{array} \right] \tag{A15}$$

$$\begin{array}{l} t_i^{41} = EI_y {\beta_1}^3 \cosh\beta_1 l_i + \overline{K} y_i \sinh\beta_1 l_i (1 + z_{\mathrm{b}} t_1),\; t_i^{42} = EI_y {\beta_1}^3 \sinh\beta_1 l_i + \overline{K} y_i \cosh\beta_1 l_i (1 + z_{\mathrm{b}} t_1) \\ t_i^{43} = EI_y {\beta_2}^3 \cosh\beta_2 l_i + \overline{K} y_i \sinh\beta_2 l_i (1 + z_{\mathrm{b}} t_2),\; t_i^{44} = EI_y {\beta_2}^3 \sinh\beta_2 l_i + \overline{K} y_i \cosh\beta_2 l_i (1 + z_{\mathrm{b}} t_2) \\ t_i^{45} = EI_y {\beta_3}^3 \cosh\beta_3 l_i + \overline{K} y_i \sinh\beta_3 l_i (1 + z_{\mathrm{b}} t_3),\; t_i^{46} = EI_y {\beta_3}^3 \sinh\beta_3 l_i + \overline{K} y_i \cosh\beta_3 l_i (1 + z_{\mathrm{b}} t_3) \\ t_i^{47} = EI_y {\beta_4}^3 \cosh\beta_4 l_i + \overline{K} y_i \sinh\beta_4 l_i (1 + z_{\mathrm{b}} t_4),\; t_i^{48} = EI_y {\beta_4}^3 \sinh\beta_4 l_i + \overline{K} y_i \cosh\beta_4 l_i (1 + z_{\mathrm{b}} t_4) \end{array}$$

$$
\mathbf{T}_{\mathrm{R}i}^{\psi} = \begin{bmatrix} 0 & t_1 & 0 & t_2 & 0 & t_3 & 0 & t_4 \\ t_1\beta_{1,i+1} & 0 & t_2\beta_{2,i+1} & 0 & t_3\beta_3 & 0 & t_4\beta_4 & 0 \\ 0 & E\Gamma_0 t_1 {\beta_{1,i+1}}^2 & 0 & E\Gamma_0 t_2 {\beta_{2,i+1}}^2 & 0 & E\Gamma_0 t_3 {\beta_3}^2 & 0 & E\Gamma_0 t_4 {\beta_4}^2 \\ E\Gamma_0 t_1 {\beta_1}^3 - GJt_1\beta_1 & 0 & E\Gamma_0 t_2 {\beta_2}^3 - GJt_2\beta_2 & 0 & E\Gamma_0 t_3 {\beta_3}^3 - GJt_3\beta_3 & 0 & E\Gamma_0 t_4 {\beta_4}^3 - GJt_4\beta_4 & 0 \end{bmatrix} \tag{A16}
$$

$$
\mathbf{T}_{\mathrm{L}i}^{\psi} = \begin{bmatrix} t_1\mathrm{sinh}\beta_1 l_i & t_1\cosh\beta_1 l_i & t_2\mathrm{sinh}\beta_2 l_i & t_2\cosh\beta_2 l_i & t_3\mathrm{sinh}\beta_3 l_i & t_3\cosh\beta_3 l_i & t_4\mathrm{sinh}\beta_4 l_i & t_4\cosh\beta_4 l_i \\ t_1\beta_1\cosh\beta_1 l_i & t_1\beta_1\mathrm{sinh}\beta_1 l_i & t_2\beta_2\cosh\beta_2 l_i & t_2\beta_2\mathrm{sinh}\beta_2 l_i & t_3\beta_3\cosh\beta_3 l_i & t_3\beta_3\mathrm{sinh}\beta_3 l_i & t_4\beta_4\cosh\beta_4 l_i & t_4\beta_4\mathrm{sinh}\beta_4 l_i \\ E\Gamma_0 t_1{\beta_1}^2\mathrm{sinh}\beta_1 l_i & E\Gamma_0 t_1{\beta_1}^2\cosh\beta_1 l_i & E\Gamma_0 t_2{\beta_2}^2\mathrm{sinh}\beta_2 l_i & E\Gamma_0 t_2{\beta_2}^2\cosh\beta_2 l_i & E\Gamma_0 t_3{\beta_3}^2\mathrm{sinh}\beta_3 l_i & E\Gamma_0 t_3{\beta_3}^2\cosh\beta_3 l_i & E\Gamma_0 t_4{\beta_4}^2\mathrm{sinh}\beta_4 l_i & E\Gamma_0 t_4{\beta_4}^2\cosh\beta_4 l_i \\ d_i^{41} & d_i^{42} & d_i^{43} & d_i^{44} & d_i^{45} & d_i^{46} & d_i^{47} & d_i^{48} \end{bmatrix} \tag{A17}
$$

$$
\begin{aligned}
d_i^{41} &= E\Gamma_0 t_1{\beta_1}^3\cosh\beta_1 l_i - GJt_1\beta_1\cosh\beta_1 l_i + z_b(1+z_b t_1)\overline{K}y_i\mathrm{sinh}\beta_1 l_i + {y_u}^2 t_1\widetilde{K}z_i\mathrm{sinh}\beta_1 l_i \\
d_i^{42} &= E\Gamma_0 t_1{\beta_1}^3\mathrm{sinh}\beta_1 l_i - GJt_1\beta_1\mathrm{sinh}\beta_1 l_i + z_b(1+z_b t_1)\overline{K}y_i\cosh\beta_1 l_i + {y_u}^2 t_1\widetilde{K}z_i\cosh\beta_1 l_i \\
d_i^{43} &= E\Gamma_0 t_2{\beta_2}^3\cosh\beta_2 l_i - GJt_2\beta_2\cosh\beta_2 l_i + z_b(1+z_b t_2)\overline{K}y_i\mathrm{sinh}\beta_2 l_i + {y_u}^2 t_2\widetilde{K}z_i\mathrm{sinh}\beta_2 l_i \\
d_i^{44} &= E\Gamma_0 t_2{\beta_2}^3\mathrm{sinh}\beta_2 l_i - GJt_2\beta_2\mathrm{sinh}\beta_2 l_i + z_b(1+z_b t_2)\overline{K}y_i\cosh\beta_2 l_i + {y_u}^2 t_2\widetilde{K}z_i\cosh\beta_2 l_i \\
d_i^{45} &= E\Gamma_0 t_3{\beta_3}^3\cosh\beta_3 l_i - GJt_3\beta_3\cosh\beta_3 l_i + z_b(1+z_b t_3)\overline{K}y_i\mathrm{sinh}\beta_3 l_i + {y_u}^2 t_3\widetilde{K}z_i\mathrm{sinh}\beta_3 l_i \\
d_i^{46} &= E\Gamma_0 t_3{\beta_3}^3\mathrm{sinh}\beta_3 l_i - GJt_3\beta_3\mathrm{sinh}\beta_3 l_i + z_b(1+z_b t_3)\overline{K}y_i\cosh\beta_3 l_i + {y_u}^2 t_3\widetilde{K}z_i\cosh\beta_3 l_i \\
d_i^{47} &= E\Gamma_0 t_4{\beta_4}^3\cosh\beta_4 l_i - GJt_4\beta_4\cosh\beta_4 l_i + z_b(1+z_b t_4)\overline{K}y_i\mathrm{sinh}\beta_4 l_i + {y_u}^2 t_4\widetilde{K}z_i\mathrm{sinh}\beta_4 l_i \\
d_i^{48} &= E\Gamma_0 t_4{\beta_4}^3\mathrm{sinh}\beta_4 l_i - GJt_4\beta_4\mathrm{sinh}\beta_4 l_i + z_b(1+z_b t_4)\overline{K}y_i\cosh\beta_4 l_i + {y_u}^2 t_4\widetilde{K}z_i\cosh\beta_4 l_i
\end{aligned}
$$

$$
\mathbf{T}_{\mathrm{L}i}^{\psi v} = \begin{bmatrix} 0 & 0 & 0 & 0 \\ 0 & 0 & 0 & 0 \\ 0 & 0 & 0 & 0 \\ \overset{\frown}{K}z_i y_u\sin\beta_5 l_i & \overset{\frown}{K}z_i y_u\cos\beta_5 l_i & \overset{\frown}{K}z_i y_u\mathrm{sinh}\beta_5 l_i & \overset{\frown}{K}z_i y_u\cosh\beta_5 l_i \end{bmatrix} \tag{A18}
$$

$$
\mathbf{T}_{\mathrm{R}i}^{v} = \begin{bmatrix} 0 & 1 & 0 & 1 \\ \beta_5 & 0 & \beta_5 & 0 \\ 0 & -{\beta_5}^2 & 0 & {\beta_5}^2 \\ -EI_Z{\beta_5}^3 & 0 & EI_Z{\beta_5}^3 & 0 \end{bmatrix} \tag{A19}
$$

$$
\mathbf{T}_{\mathrm{L}i}^{v} = \begin{bmatrix} \sin\beta_5 l_i & \cos\beta_5 l_i & \mathrm{sinh}\beta_5 l_i & \cosh\beta_5 l_i \\ \beta_5\cos\beta_5 l_i & -\beta_5\sin\beta_5 l_i & \beta_5\cosh\beta_5 l_i & \beta_5\mathrm{sinh}\beta_5 l_i \\ -{\beta_5}^2\sin\beta_5 l_i & -{\beta_5}^2\cos\beta_5 l_i & {\beta_5}^2\mathrm{sinh}\beta_5 l_i & {\beta_5}^2\cosh\beta_5 l_i \\ \begin{matrix} -EI_Z{\beta_5}^3\cos\beta_5 l_i \\ +\overline{K}z_i\sin\beta_5 l_i \end{matrix} & \begin{matrix} EI_Z{\beta_5}^3\sin\beta_5 l_i \\ +\overline{K}z_i\cos\beta_5 l_i \end{matrix} & \begin{matrix} EI_Z{\beta_5}^3\cosh\beta_5 l_i \\ +\overline{K}z_i\mathrm{sinh}\beta_5 l_i \end{matrix} & \begin{matrix} EI_Z{\beta_5}^3\mathrm{sinh}\beta_5 l_i \\ +\overline{K}z_i\cosh\beta_5 l_i \end{matrix} \end{bmatrix} \tag{A20}
$$

$$
\mathbf{T}_{\mathrm{L}i}^{v\psi} = \begin{bmatrix} 0 & 0 & 0 & 0 & 0 & 0 & 0 & 0 \\ 0 & 0 & 0 & 0 & 0 & 0 & 0 & 0 \\ 0 & 0 & 0 & 0 & 0 & 0 & 0 & 0 \\ \hat{K}z_i y_u t_1\mathrm{sinh}\beta_1 l_i & \hat{K}z_i y_u t_1\cosh\beta_1 l_i & \hat{K}z_i y_u t_2\mathrm{sinh}\beta_2 l_i & \hat{K}z_i y_u t_2\cosh\beta_2 l_i & \hat{K}z_i y_u t_3\mathrm{sinh}\beta_3 l_i & \hat{K}z_i y_u t_3\cosh\beta_3 l_i & \hat{K}z_i y_u t_4\mathrm{sinh}\beta_4 l_i & \hat{K}z_i y_u t_4\cosh\beta_4 l_i \end{bmatrix} \tag{A21}
$$

Appendix C. The Derivations of $\mathbf{B}_\mathbf{L}$ and $\mathbf{B}_\mathbf{R}$

Some possibly complicated boundaries, such as an elastically supported, lumped mass, rotational inertia boundary, or any combination, can be given in a general way as

$$\begin{aligned} M^w(0) &= -(K^w_{LT} + C^w_{LT}\overline{\omega} + J^w_{\mathrm{L}}\overline{\omega}^2)W'(0)\ M^w(L) = (K^w_{RT} + C^w_{\mathrm{RT}}\overline{\omega} + J^w_{\mathrm{R}}\overline{\omega}^2)W'(L) \\ S^w(0) &= -(K^w_{\mathrm{L}} + C^w_{\mathrm{L}}\overline{\omega} + m_{\mathrm{L}}\overline{\omega}^2)W(0)\ S^w(L) = (K^w_{\mathrm{R}} + C^w_{\mathrm{R}}\overline{\omega} + m_{\mathrm{R}}\overline{\omega}^2)W(L) \end{aligned} \tag{A22}$$

$$\begin{aligned} M^v(0) &= -(K^v_{\mathrm{LT}} + C^v_{\mathrm{LT}}\overline{\omega} + J^v_{\mathrm{L}}\overline{\omega}^2)V'(0)\ M^v(L) = (K^v_{\mathrm{RT}} + C^v_{\mathrm{RT}}\overline{\omega} + J^v_{\mathrm{R}}\overline{\omega}^2)V'(L) \\ S^v(0) &= -(K^v_{\mathrm{L}} + C^v_{\mathrm{L}}\overline{\omega} + m_{\mathrm{L}}\overline{\omega}^2)W(0)\ S^v(L) = (K^v_{\mathrm{R}} + C^v_{\mathrm{R}}\overline{\omega} + m_{\mathrm{R}}\overline{\omega}^2)W(L) \end{aligned} \tag{A23}$$

$$\begin{aligned} &B(0) = 0\ B(L) = 0 \\ &T(0) = -(K^\psi_{\mathrm{LT}} + C^\psi_{\mathrm{LT}}\overline{\omega} + J^\psi_{\mathrm{L}}\overline{\omega}^2)\Psi(0)\ T(L) = (K^\psi_{\mathrm{RT}} + C^\psi_{\mathrm{RT}}\overline{\omega} + J^\psi_{\mathrm{R}}\overline{\omega}^2)\Psi(L) \end{aligned} \tag{A24}$$

where K^w_{L}, K^w_{R}, K^w_{LT}, K^w_{RT} and C^w_{L}, C^w_{R}, C^w_{LT}, C^w_{RT} and K^v_{L}, K^w_{R}, K^w_{LT}, K^w_{RT} and C^w_{L}, C^w_{R}, C^w_{LT}, C^w_{RT} are, respectively the translational and rotational stiffness and damping of lumped attachment at the left and right end of the thin-walled beam in the w and v direction; m_{L}, m_{R} and J^w_{L}, J^w_{R} and J^v_{L}, J^v_{R} are the corresponding mass and moment of inertia. K^ψ_{LT}, K^ψ_{RT} and C^ψ_{LT}, C^ψ_{RT} and J^ψ_{LT}, J^ψ_{RT} are the rotational stiffness, damping and moment of inertia of lumped attachment at the left and right end of the thin-walled beam in ψ direction respectively.

Substituting Equations (22)–(35) into Equations (A22)–(A24) and organizing them in matrix form, one obtains:

$$\mathbf{B}^w_{\mathrm{L}}\boldsymbol{C}^w_1 = \{0\}_{8\times 1} \tag{A25}$$

where

$$\mathbf{B}^w_{\mathrm{L}} = \begin{bmatrix} Ke^w_{LT}\beta_1 & EI_y\beta_1{}^2 & Ke^w_{LT}\beta_2 & EI_y\beta_2{}^2 & Ke^w_{LT}\beta_3 & EI_y\beta_3{}^2 & Ke^w_{LT}\beta_4 & EI_y\beta_4{}^2 \\ EI_y\beta_1{}^3 & Ke^w_{\mathrm{L}} & EI_y\beta_2{}^3 & Ke^w_{\mathrm{L}} & EI_y\beta_3{}^3 & Ke^w_{\mathrm{L}} & EI_y\beta_4{}^3 & Ke^w_{\mathrm{L}} \end{bmatrix} \tag{A26}$$

with $Ke^w_{\mathrm{LT}} = K^w_{\mathrm{LT}} + C^w_{\mathrm{LT}}\overline{\omega} + J^w_{\mathrm{L}}\overline{\omega}^2\ Ke^w_{\mathrm{L}} = K^w_{\mathrm{L}} + C^w_{\mathrm{L}}\overline{\omega} + m_{\mathrm{L}}\overline{\omega}^2$

$$\mathbf{B}^\psi_{\mathrm{L}}\boldsymbol{C}^\psi_1 = \{0\}_{8\times 1} \tag{A27}$$

where

$$\mathbf{B}^\psi_{\mathrm{L}} = \begin{bmatrix} 0 & E\Gamma_0 t_1\beta_1{}^2 & 0 & E\Gamma_0 t_2\beta_2{}^2 & 0_3 & E\Gamma_0 t_3\beta_3{}^2 & 0 & E\Gamma_0 t_4\beta_4{}^2 \\ b^\psi_{\mathrm{L21}} & b^\psi_{\mathrm{L21}} & b^\psi_{\mathrm{L21}} & b^\psi_{\mathrm{L21}} & b^\psi_{\mathrm{L21}} & b^\psi_{\mathrm{L21}} & b^\psi_{\mathrm{L21}} & b^\psi_{\mathrm{L21}} \end{bmatrix} \tag{A28}$$

with

$$\begin{aligned} &b^\psi_{\mathrm{L21}} = (E\Gamma_0\beta_1{}^3 - GJ\beta_1)t_1\ b^\psi_{\mathrm{L22}} = Ke^\psi_{\mathrm{L}}t_1\ b^\psi_{\mathrm{L23}} = (E\Gamma_0\beta_2{}^3 - GJ\beta_2)t_2\ b^\psi_{\mathrm{L24}} = Ke^\psi_{\mathrm{L}}t_2 \\ &b^\psi_{\mathrm{L25}} = (E\Gamma_0\beta_3{}^3 - GJ\beta_3)t_3\ b^\psi_{\mathrm{L26}} = Ke^\psi_{\mathrm{L}}t_3\ b^\psi_{\mathrm{L27}} = (E\Gamma_0\beta_4{}^3 - GJ\beta_4)t_4\ b^\psi_{\mathrm{L28}} = Ke^\psi_{\mathrm{L}}t_4 \end{aligned}$$

and $Ke^\psi_{\mathrm{LT}} = K^\psi_{\mathrm{LT}} + C^\psi_{\mathrm{LT}}\overline{\omega} + J^\psi_{\mathrm{L}}\overline{\omega}^2$

$$\mathbf{B}^v_{\mathrm{L}}\boldsymbol{C}^v_1 = \{0\}_{4\times 1} \tag{A29}$$

where

$$\mathbf{B}^v_{\mathrm{L}} = \begin{bmatrix} Ke^v_{\mathrm{LT}}\beta_5 & -EI_z\beta_5{}^2 & Ke^v_{\mathrm{LT}}\beta_5 & EI_z\beta_5{}^2 \\ -EI_z\beta_5{}^3 & Ke^v_{\mathrm{L}} & EI_z\beta_5{}^3 & Ke^v_{\mathrm{L}} \end{bmatrix} \tag{A30}$$

with $Ke^v_{\mathrm{LT}} = K^v_{\mathrm{LT}} + C^v_{\mathrm{LT}}\overline{\omega} + J^v_{\mathrm{L}}\overline{\omega}^2\ Ke^v_{\mathrm{L}} = K^v_{\mathrm{L}} + C^v_{\mathrm{L}}\overline{\omega} + m_{\mathrm{L}}\overline{\omega}^2$

$$\mathbf{B}^w_{\mathrm{R}}\boldsymbol{C}^w_{N+1} = \{0\}_{8\times 1} \tag{A31}$$

where

$$\mathbf{B}^w_{\mathrm{R}} = \begin{bmatrix} b^w_{\mathrm{R11}} & b^w_{\mathrm{R12}} & b^w_{\mathrm{R13}} & b^w_{\mathrm{R14}} & b^w_{\mathrm{R15}} & b^w_{\mathrm{R16}} & b^w_{\mathrm{R17}} & b^w_{\mathrm{R18}} \\ b^w_{\mathrm{R21}} & b^w_{\mathrm{R21}} & b^w_{\mathrm{R21}} & b^w_{\mathrm{R21}} & b^w_{\mathrm{R21}} & b^w_{\mathrm{R21}} & b^w_{\mathrm{R21}} & b^w_{\mathrm{R21}} \end{bmatrix} \tag{A32}$$

with

$$
\begin{aligned}
b^w_{\mathrm{R}11} &= EI_y\beta_1{}^2\sinh\beta_1 l_{N+1} - Ke^w_{\mathrm{RT}}\beta_1\cosh\beta_1 l_{N+1},\ b^w_{\mathrm{R}12} = EI_y\beta_1{}^2\cosh\beta_1 l_{N+1} - Ke^w_{\mathrm{RT}}\beta_1\sin\beta_1 l_{N+1}\\
b^w_{\mathrm{R}13} &= EI_y\beta_2{}^2\sinh\beta_2 l_{N+1} - Ke^w_{\mathrm{RT}}\beta_2\cosh\beta_2 l_{N+1},\ b^w_{\mathrm{R}14} = EI_y\beta_2{}^2\cosh\beta_2 l_{N+1} - Ke^w_{\mathrm{RT}}\beta_2\sin\beta_1 l_{N+1}\\
b^w_{\mathrm{R}15} &= EI_y\beta_3{}^2\sinh\beta_3 l_{N+1} - Ke^w_{\mathrm{RT}}\beta_3\cosh\beta_3 l_{N+1},\ b^w_{\mathrm{R}16} = EI_y\beta_3{}^2\cosh\beta_3 l_{N+1} - Ke^w_{\mathrm{RT}}\beta_3\sin\beta_3 l_{N+1}\\
b^w_{\mathrm{R}17} &= EI_y\beta_4{}^2\sinh\beta_4 l_{N+1} - Ke^w_{\mathrm{RT}}\beta_4\cosh\beta_4 l_{N+1},\ b^w_{\mathrm{R}18} = EI_y\beta_4{}^2\cosh\beta_4 l_{N+1} - Ke^w_{\mathrm{RT}}\beta_4\sin\beta_4 l_{N+1}\\
b^w_{\mathrm{R}21} &= EI_y\beta_1{}^3\cosh\beta_1 l_{N+1} - Ke^w_{\mathrm{R}}\sinh\beta_1 l_{N+1}, b^w_{\mathrm{R}22} = EI_y\beta_1{}^3\sinh\beta_1 l_{N+1} - Ke^w_{\mathrm{R}}\cosh\beta_1 l_{N+1}\\
b^w_{\mathrm{R}23} &= EI_y\beta_2{}^3\cosh\beta_2 l_{N+1} - Ke^w_{\mathrm{R}}\sinh\beta_2 l_{N+1}, b^w_{\mathrm{R}24} = EI_y\beta_2{}^3\sinh\beta_2 l_{N+1} - Ke^w_{\mathrm{R}}\cosh\beta_2 l_{N+1}\\
b^w_{\mathrm{R}25} &= EI_y\beta_3{}^3\cosh\beta_3 l_{N+1} - Ke^w_{\mathrm{R}}\sinh\beta_3 l_{N+1}, b^w_{\mathrm{R}26} = EI_y\beta_3{}^3\sinh\beta_3 l_{N+1} - Ke^w_{\mathrm{R}}\cosh\beta_3 l_{N+1}\\
b^w_{\mathrm{R}27} &= EI_y\beta_4{}^3\cosh\beta_4 l_{N+1} - Ke^w_{\mathrm{R}}\sinh\beta_4 l_{N+1}, b^w_{\mathrm{R}28} = EI_y\beta_4{}^3\sinh\beta_4 l_{N+1} - Ke^w_{\mathrm{R}}\cosh\beta_4 l_{N+1}
\end{aligned}
$$

and $Ke^w_{\mathrm{LT}} = K^w_{\mathrm{LT}} + C^w_{\mathrm{LT}}\overline{\omega} + J^w\overline{\omega}^2\ Ke^w_{\mathrm{L}} = K^w_{\mathrm{L}} + C^w_{\mathrm{L}}\overline{\omega} + m\overline{\omega}^2$

$$\mathbf{B}^\psi_{\mathrm{R}}\boldsymbol{C}^\psi_{N+1} = \{0\}_{8\times 1} \tag{A33}$$

where

$$\mathbf{B}^\psi_{\mathrm{R}} = \begin{bmatrix} b^\psi_{\mathrm{R}11} & b^\psi_{\mathrm{R}12} & b^\psi_{\mathrm{R}13} & b^\psi_{\mathrm{R}14} & b^\psi_{\mathrm{R}15} & b^\psi_{\mathrm{R}16} & b^\psi_{\mathrm{R}17} & b^\psi_{\mathrm{R}18} \\ b^\psi_{\mathrm{R}21} & b^\psi_{\mathrm{R}21} & b^\psi_{\mathrm{R}21} & b^\psi_{\mathrm{R}21} & b^\psi_{\mathrm{R}21} & b^\psi_{\mathrm{R}21} & b^\psi_{\mathrm{R}21} & b^\psi_{\mathrm{R}21} \end{bmatrix} \tag{A34}$$

with

$$
\begin{aligned}
b^\psi_{\mathrm{R}11} &= E\Gamma_0\beta_1{}^2 t_1\sinh\beta_1 l_{N+1},\ b^\psi_{\mathrm{R}12} = E\Gamma_0\beta_1{}^2 t_1\cosh\beta_1 l_{N+1}, b^\psi_{\mathrm{R}13} = E\Gamma_0\beta_2{}^2 t_2\sinh\beta_2 l_{N+1},\ b^\psi_{\mathrm{R}14} = E\Gamma_0\beta_2{}^2 t_2\cosh\beta_2 l_{N+1}\\
b^\psi_{\mathrm{R}15} &= E\Gamma_0\beta_3{}^2 t_3\sinh\beta_3 l_{N+1},\ b^\psi_{\mathrm{R}16} = E\Gamma_0\beta_3{}^2 t_3\cosh\beta_3 l_{N+1}, b^\psi_{\mathrm{R}17} = E\Gamma_0\beta_4{}^2 t_4\sinh\beta_4 l_{N+1},\ b^\psi_{\mathrm{R}18} = E\Gamma_0\beta_4{}^2 t_4\cosh\beta_4 l_{N+1}\\
b^\psi_{\mathrm{R}21} &= (E\Gamma_0\beta_1{}^3 - GJ\beta_1)t_1\cosh\beta_1 l_{N+1} - Ke^w_{\mathrm{RT}}t_1\sinh\beta_1 l_{N+1}, b^w_{\mathrm{R}21} = (E\Gamma_0\beta_1{}^3 - GJ\beta_1)t_1\sinh\beta_1 l_{N+1} - Ke^w_{\mathrm{RT}}t_1\cosh\beta_1 l_{N+1}\\
b^w_{\mathrm{R}23} &= (E\Gamma_0\beta_2{}^3 - GJ\beta_2)t_2\cosh\beta_2 l_{N+1} - Ke^w_{\mathrm{RT}}t_2\sinh\beta_2 l_{N+1}, b^w_{\mathrm{R}23} = (E\Gamma_0\beta_2{}^3 - GJ\beta_2)t_2\sinh\beta_2 l_{N+1} - Ke^w_{\mathrm{RT}}t_2\cosh\beta_2 l_{N+1}\\
b^w_{\mathrm{R}25} &= (E\Gamma_0\beta_3{}^3 - GJ\beta_3)t_3\cosh\beta_3 l_{N+1} - Ke^w_{\mathrm{RT}}t_3\sinh\beta_3 l_{N+1}, b^w_{\mathrm{R}23} = (E\Gamma_0\beta_3{}^3 - GJ\beta_3)t_3\sinh\beta_3 l_{N+1} - Ke^w_{\mathrm{RT}}t_3\cosh\beta_3 l_{N+1}\\
b^w_{\mathrm{R}25} &= (E\Gamma_0\beta_4{}^3 - GJ\beta_4)t_4\cosh\beta_4 l_{N+1} - Ke^w_{\mathrm{RT}}t_4\sinh\beta_4 l_{N+1}, b^w_{\mathrm{R}23} = (E\Gamma_0\beta_4{}^3 - GJ\beta_4)t_4\sinh\beta_4 l_{N+1} - Ke^w_{\mathrm{RT}}t_4\cosh\beta_4 l_{N+1}
\end{aligned}
$$

and $Ke^\psi_{\mathrm{RT}} = K^\psi_{\mathrm{RT}} + C^\psi_{\mathrm{RT}}\overline{\omega} + J^\psi_{\mathrm{R}}\overline{\omega}^2$

$$\mathbf{B}^v_{\mathrm{R}}\boldsymbol{C}^v_{N+1} = \{0\}_{4\times 1} \tag{A35}$$

where

$$\mathbf{B}^v_{\mathrm{R}} = \begin{bmatrix} -EI_z\beta_5^2\sin(\beta_5 l_{N+1}) - Ke^v_{\mathrm{LT}}\beta_5\cos\beta_5 l_{N+1} & -EI_z\beta_5^2\cos(\beta_5 l_{N+1}) - Ke^v_{\mathrm{LT}}\beta_5\sin\beta_5 l_{N+1} \\ -EI_z\beta_5^3\cos\beta_5 l_{N+1} - Ke^v_{\mathrm{L}}\sin\beta_5 l_{N+1} & EI_z\beta_5^3\sin\beta_5 l_{N+1} - Ke^v_{\mathrm{L}}\cos\beta_5 l_{N+1} \\ EI_z\beta_5^2\sinh(\beta_5 l_{N+1}) - Ke^v_{\mathrm{LT}}\beta_5\cosh\beta_5 l_{N+1} & EI_z\beta_5{}^2\cosh(\beta_5 l_{N+1}) - Ke^v_{\mathrm{LT}}\beta_5\sinh\beta_5 l_{N+1} \\ EI_z\beta_5{}^3\cosh\beta_5 l_{N+1} - Ke^v_{\mathrm{L}}\sinh\beta_5 l_{N+1} & EI_z\beta_5{}^3\sinh\beta_5 l_{N+1} - Ke^v_{\mathrm{L}}\cosh\beta_5 l_{N+1} \end{bmatrix} \tag{A36}$$

with $Ke^v_{\mathrm{RT}} = K^v_{\mathrm{RT}} + C^v_{\mathrm{RT}}\overline{\omega} + J^v_{\mathrm{R}}\overline{\omega}^2\ Ke^v_{\mathrm{R}} = K^v_{\mathrm{R}} + C^v_{\mathrm{R}}\overline{\omega} + m_{\mathrm{R}}\overline{\omega}^2$.

For the other usually used boundary, one can easily derive the corresponding coefficient matrices through the similar procedure.

Combing Equations (A25), (A27) and (A29) and organizing them in matrix form, one obtains the coefficient matrices associated with the left end $\mathbf{B}_{\mathrm{L}}$:

$$\begin{bmatrix} \mathbf{B}^w_{\mathrm{L}} & 0_{2\times 4} \\ \mathbf{B}^\psi_{\mathrm{L}} & 0_{2\times 4} \\ 0_{2\times 8} & \mathbf{B}^v_{\mathrm{L}} \end{bmatrix} \begin{bmatrix} \boldsymbol{C}^w_1 \\ \boldsymbol{C}^v_1 \end{bmatrix} = \mathbf{B}_{\mathrm{L}\,6\times 12} \begin{bmatrix} \boldsymbol{C}^w_1 \\ \boldsymbol{C}^v_1 \end{bmatrix} = [0]_{6\times 1} \tag{A37}$$

Similarly, the combination of Equations (A31), (A33) and (A35) can show the coefficient matrices associated with the right end $\mathbf{B}_{\mathrm{R}}$:

$$\begin{bmatrix} \mathbf{B}^w_{\mathrm{R}} & 0_{2\times 4} \\ \mathbf{B}^\psi_{\mathrm{R}} & 0_{2\times 4} \\ 0_{2\times 8} & \mathbf{B}^v_{\mathrm{R}} \end{bmatrix} \begin{bmatrix} \boldsymbol{C}^w_{N+1} \\ \boldsymbol{C}^v_{N+1} \end{bmatrix} = \mathrm{B}_{\mathrm{R}6\times 12}\mathbf{H}_{12\times 12} \begin{bmatrix} \boldsymbol{C}^w_1 \\ \boldsymbol{C}^v_1 \end{bmatrix} = [0]_{6\times 1} \tag{A38}$$

Appendix D. The Expressions of the Derivative Matrices $\mathbf{T}^w$, $\mathbf{T}^\psi$ and $\mathbf{T}^v$

$$\begin{bmatrix} \mathbf{B}_\mathrm{L}^w & 0_{2\times4} \\ \mathbf{B}_\mathrm{L}^\psi & 0_{2\times4} \\ 0_{2\times8} & \mathbf{B}_\mathrm{L}^v \end{bmatrix} \begin{bmatrix} C_1^w \\ C_1^v \end{bmatrix} = \mathbf{B}_{\mathrm{L}\,6\times12} \begin{bmatrix} C_1^w \\ C_1^v \end{bmatrix} = [0]_{6\times1} \tag{A39}$$

$$\mathbf{T}_{m,1}^{w,2} = \begin{bmatrix} \sinh\beta_1 l_{m,1} & \cosh\beta_1 l_{m,1} & \sinh\beta_2 l_{m,1} & \cosh\beta_2 l_{m,1} \\ \beta_1\cosh\beta_1 l_{m,1} & \beta_1\sinh\beta_1 l_{m,1} & \beta_2\cosh\beta_2 l_{m,1} & \beta_2\sinh\beta_2 l_{m,1} \\ {\beta_1}^2\sinh\beta_1 l_{m,1} & {\beta_1}^2\cosh\beta_1 l_{m,1} & {\beta_2}^2\sinh\beta_2 l_{m,1} & {\beta_2}^2\cosh h\beta_2 l_{m,1} \\ EI_y{\beta_1}^3\cosh\beta_1 l_{m,1} & EI_y{\beta_1}^3\sinh\beta_1 l_{m,1} & EI_y{\beta_2}^3\cosh\beta_2 l_{m,1} & EI_y{\beta_2}^3\sinh\beta_2 l_{m,1} \end{bmatrix.} \\ \begin{bmatrix.} \sinh\beta_3 l_{m,1} & \cosh\beta_3 l_{m,1} & \sinh\beta_4 l_{m,1} & \cosh\beta_4 l_{m,1} \\ \beta_3\cosh\beta_3 l_{m,1} & \beta_3\sinh\beta_3 l_{m,1} & \beta_4\cosh\beta_4 l_{m,1} & \beta_4\sinh\beta_4 l_{m,1} \\ {\beta_3}^2\sinh\beta_3 l_{m,1} & {\beta_3}^2\cosh\beta_3 l_{m,1} & {\beta_4}^2\sinh\beta_4 l_{m,1} & {\beta_4}^2\cosh\beta_4 l_{m,1} \\ EI_y{\beta_3}^3\cosh\beta_3 l_{m,1} & EI_y{\beta_1}^3\sinh\beta_3 l_{m,1} & EI_y{\beta_4}^3\cosh\beta_4 l_{m,1} & EI_y{\beta_4}^3\sinh\beta_4 l_{m,1} \end{bmatrix} \tag{A40}$$

$$\mathbf{T}_{m,2}^{\psi,1} = \begin{bmatrix} 0 & t_1 & 0 & t_2 \\ t_1\beta_1 & 0 & t_2\beta_2 & 0 \\ 0 & E\Gamma_0 t_1{\beta_1}^2 & 0 & E\Gamma_0 t_2{\beta_2}^2 \\ E\Gamma_0 t_1{\beta_1}^3 - GJt_1{\beta_1}^3 & 0 & E\Gamma_0 t_2{\beta_2}^3 - GJt_2{\beta_2}^3 & 0 \end{bmatrix.} \\ \begin{bmatrix.} 0 & t_3 & 0 & t_4 \\ t_3\beta_3 & 0 & t_4\beta_4 & 0 \\ 0 & E\Gamma_0 t_3{\beta_3}^2 & 0 & E\Gamma_0 t_4{\beta_4}^2 \\ E\Gamma_0 t_3{\beta_3}^3 - GJt_3{\beta_3}^3 & 0 & E\Gamma_0 t_4{\beta_4}^3 - GJt_4{\beta_4}^3 & 0 \end{bmatrix} \tag{A41}$$

$$\mathbf{T}_{m,1}^{\psi,2} = \begin{bmatrix} t_1\sinh\beta_1 l_{m,1} & t_1\cosh\beta_1 l_{m,1} & t_2\sinh\beta_2 l_{m,1} & t_2\cosh\beta_2 l_{m,1} \\ t_1\beta_1\cosh\beta_1 l_{m,1} & t_1\beta_1\sinh\beta_1 l_{m,1} & t_2\beta_2\cosh\beta_2 l_{m,1} & t_2\beta_2\sinh\beta_2 l_{m,1} \\ E\Gamma_0 t_1{\beta_1}^2\sinh\beta_1 l_{m,1} & E\Gamma_0 t_1{\beta_1}^2\cosh\beta_1 l_{m,1} & E\Gamma_0 t_2{\beta_2}^2\sinh\beta_2 l_{m,1} & E\Gamma_0 t_2{\beta_2}^2\cosh\beta_2 l_{m,1} \\ d_{m,1}^{41} & d_{m,1}^{42} & d_{m,1}^{43} & d_{m,1}^{44} \end{bmatrix.} \\ \begin{bmatrix.} t_3\sinh\beta_3 l_{m,1} & t_3\cosh\beta_3 l_{m,1} & t_4\sinh\beta_4 l_{m,1} & t_4\cosh\beta_4 l_{m,1} \\ t_3\beta_3\cosh\beta_3 l_{m,1} & t_3\beta_3\sinh\beta_3 l_{m,1} & t_4\beta_4\cosh\beta_4 l_{m,1} & t_4\beta_4\sinh\beta_4 l_{m,1} \\ E\Gamma_0 t_3{\beta_3}^2\sinh\beta_3 l_{m,1} & E\Gamma_0 t_3{\beta_3}^2\cosh\beta_3 l_{m,1} & E\Gamma_0 t_4{\beta_4}^2\sinh\beta_4 l_{m,1} & E\Gamma_0 t_4{\beta_4}^2\cosh\beta_4 l_{m,1} \\ d_{m,1}^{45} & d_{m,1}^{46} & d_{m,1}^{47} & d_{m,1}^{48} \end{bmatrix} \tag{A42}$$

with

$$\begin{aligned} d_{m,1}^{41} &= E\Gamma_0 t_1\beta_1^3\cosh\beta_1 l_{m,1} - GJt_1\beta_1\cosh\beta_1 l_{m,1}; d_{m,1}^{42} = E\Gamma_0 t_1\beta_1^3\sinh\beta_1 l_{m,1} - GJt_1\beta_1\sinh\beta_1 l_{m,1} \\ d_{m,1}^{43} &= E\Gamma_0 t_2\beta_2^3\cosh\beta_2 l_{m,1} - GJt_2\beta_2\cosh\beta_2 l_{m,1}; d_{m,1}^{44} = E\Gamma_0 t_2\beta_2^3\sinh\beta_2 l_{m,1} - GJt_2\beta_2\sinh\beta_2 l_{m,1} \\ d_{m,1}^{45} &= E\Gamma_0 t_3\beta_3^3\cosh\beta_3 l_{m,1} - GJt_{m,1}^3\beta_3\cosh\beta_3 l_{m,1}; d_{m,1}^{46} = E\Gamma_0 t_3\beta_3^3\sinh\beta_3 l_{m,1} - GJt_3\beta_3\sinh\beta_3 l_{m,1} \\ d_{m,1}^{47} &= E\Gamma_0 t_4\beta_4^3\cosh\beta_4 l_{m,1} - GJt_4\beta_4\cosh\beta_4 l_{m,1}; d_{m,1}^{48} = E\Gamma_0 t_4{\beta_4}^3\sinh\beta_4 l_{m,1} - GJt_4\beta_4\sinh\beta_4 l_{m,1} \end{aligned}$$

$$\mathbf{T}_{m,2}^{v,1} = \begin{bmatrix} 0 & 1 & 0 & 1 \\ \beta_5 & 0 & \beta_5 & 0 \\ 0 & -{\beta_5}^2 & 0 & {\beta_5}^2 \\ -EI_Z{\beta_5}^3 & 0 & EI_Z{\beta_5}^3 & 0 \end{bmatrix} \tag{A43}$$

$$\mathbf{T}_{m,1}^{v,2} = \begin{bmatrix} \sin\beta_5 l_{m,1} & \cos\beta_5 l_{m,1} & \sinh\beta_5 l_{m,1} & \cosh\beta_5 l_{m,1} \\ \beta_5\cos\beta_5 l_{m,1} & -\beta_5\sin\beta_5 l_{m,1} & \beta_5\cosh\beta_5 l_{m,1} & \beta_5\sinh\beta_5 l_{m,1} \\ -{\beta_5}^2\sin\beta_5 l_{m,1} & -{\beta_5}^2\cos\beta_5 l_{m,1} & {\beta_5}^2\sinh\beta_5 l_{m,1} & {\beta_5}^2\cosh\beta_5 l_{m,1} \\ -EI_Z{\beta_5}^3\cos\beta_5 l_{m,1} & EI_Z{\beta_5}^3\sin\beta_5 l_{m,1} & EI_Z{\beta_5}^3\cosh\beta_5 l_{m,1} & EI_Z{\beta_5}^3\cosh\beta_5 l_{m,1} \end{bmatrix} \tag{A44}$$

Appendix E

The stiffness matrix [**Ke**], mass matrix [**Me**] and the damping matrix [**Ce**] of the constrained thin-walled beam element illustrated in Figure 2 can be given by Equations (A45)–(A47). In the matrixes, the coefficients Meij and Keij (*i*,*j* = 1–6) are, respectively, equal to those of the mass matrix and stiffness matrix for an unconstrained beam element. One can find their values from the general textbooks. i and n donate the serial number of the subsystem and thin-walled beam element respectively, N is the total number of thin-walled beam elements.

$$[\mathbf{Ke}] = \begin{array}{c} \begin{matrix} \cdots & v_{6n-5} & v_{6n-4} & v_{6n-3} & v_{6n-2} & v_{6n-1} & v_{6n} & \cdots & v_{6(N+1)+1} & v_{6(N+1)+2} & v_{6(N+1)+3} & \cdots \end{matrix} \\ \begin{bmatrix} \vdots & & & & & & & & & \\ \begin{matrix} K^n_{e11}+ \\ k^L_{z,i}+k^R_{z,i} \end{matrix} & K^n_{e12} & \begin{matrix} K^n_{e13}+ \\ (k^R_{z,i}-k^L_{z,i})y_i \end{matrix} & K^n_{e14} & K^n_{e15} & K^n_{e16} & & -(k^L_{z,i}+k^R_{z,i}) & & k^L_{z,i}l^L_i-k^R_{z,i}l^R_i & \\ K^n_{e21} & \begin{matrix} K^n_{e22} \\ +k^L_{y,i}+k^R_{y,i} \end{matrix} & \begin{matrix} K^n_{e23} \\ (k^L_{y,i}+k^R_{y,i})z_b \end{matrix} & K^n_{e24} & K^n_{e25} & K^n_{e26} & & & -(k^L_{y,i}+k^R_{y,i}) & & \\ \begin{matrix} K^n_{e31}+ \\ (k^R_{z,i}-k^L_{z,i})y_u \end{matrix} & \begin{matrix} K^n_{e32}+ \\ (k^L_{y,i}+k^R_{y,i})z_b \end{matrix} & \begin{matrix} K^n_{e33}+(k^L_{z,i}+k^R_{z,i}){y_u}^2 \\ +(k^L_{y,i}+k^R_{y,i}){z_b}^2 \end{matrix} & K^n_{e34} & K^n_{e35} & K^n_{e36} & & (-k^R_{z,i}+k^L_{z,i})y_u & -(k^L_{y,i}+k^R_{y,i})z_b & -(k^L_{z,i}l^L_i+k^R_{z,i}l^R_i)y_u & \\ K^n_{e41} & K^n_{e42} & K^n_{e43} & K^n_{e44} & K^n_{e45} & K^n_{e46} & & & & & \\ K^n_{e51} & K^n_{e52} & K^n_{e53} & K^n_{e54} & K^n_{e55} & K^n_{e56} & & & & & \\ K^n_{e61} & K^n_{e62} & K^n_{e63} & K^n_{e64} & K^n_{e65} & K^n_{e66} & & & & & \\ & & & & & & \vdots & & & & \\ -(k^L_{z,i}+k^R_{z,i}) & & (k^L_{z,i}-k^R_{z,i})y_u & & & & & k^L_{z,i}+k^R_{z,i} & & -k^L_{z,i}l^L_i+k^R_{z,i}l^R_i & \\ & -(k^L_{y,i}+k^R_{y,i}) & -(k^L_{y,i}+k^R_{y,i})z_b & & & & & & k^L_{y,i}+k^R_{y,i} & & \\ k^L_{z,i}l^L_i-k^R_{z,i}l^R_i & & -(k^L_{z,i}l^L_i+k^R_{z,i}l^R_i)y_u & & & & & k^R_{z,i}l^R_i-k^L_{z,i}l^L_i & & k^L_{z,i}l^{L2}_i+k^R_{z,i}l^{R2}_i & \\ & & & & & & & & & & \vdots \end{bmatrix} \end{array} \begin{matrix} \vdots \\ v_{6n-5} \\ v_{6n-4} \\ v_{6n-3} \\ v \;\; 6n-2 \\ v \;\; 6n-1 \\ v_{6n} \\ \vdots \\ v_{6(N+1)+1} \\ v_{6(N+1)+2} \\ v_{6(N+1)+3} \end{matrix} \qquad \text{(A45)}$$

$$
[\mathbf{Me}] = \begin{array}{cc}
\begin{array}{cccccccccccc} \cdots & v_{6n-5} & v_{6n-4} & v_{6n-3} & v_{6n-2} & v_{6n-1} & v_{6n} & \cdots & v_{6(N+1)+1} & v_{6(N+1)+2} & v_{6(N+1)+3} & \cdots \end{array} & \\
\begin{bmatrix}
\vdots & & & & & & & & & & & \\
 & M^n_{e11} & M^n_{e12} & M^n_{e13} & M^n_{e14} & M^n_{e15} & M^n_{e16} & & & & & \\
 & M^n_{e21} & M^n_{e22} & M^n_{e23} & M^n_{e24} & M^n_{e25} & M^n_{e26} & & & & & \\
 & M^n_{e31} & M^n_{e32} & M^n_{e33} & M^n_{e34} & M^n_{e35} & M^n_{e36} & & & & & \\
 & M^n_{e41} & M^n_{e42} & M^n_{e43} & M^n_{e44} & M^n_{e45} & M^n_{e46} & & & & & \\
 & M^n_{e51} & M^n_{e52} & M^n_{e53} & M^n_{e54} & M^n_{e55} & M^n_{e56} & & & & & \\
 & M^n_{e61} & M^n_{e62} & M^n_{e63} & M^n_{e64} & M^n_{e65} & M^n_{e66} & & & & & \\
 & & & & & & & \vdots & & & & \\
 & & & & & & & & m_i & & & \\
 & & & & & & & & & m_i & & \\
 & & & & & & & & & & J_i & \\
 & & & & & & & & & & & \vdots
\end{bmatrix} &
\begin{array}{c} \vdots \\ v_{6n-5} \\ v_{6n-4} \\ v_{6n-3} \\ v_{6n-2} \\ v_{6n-1} \\ v_{6n} \\ \vdots \\ v_{6(N+1)+1} \\ v_{6(N+1)+2} \\ v_{6(N+1)+3} \\ \vdots \end{array}
\end{array} \tag{A46}
$$

$$
[\mathbf{Ce}] = \begin{array}{cc}
\begin{array}{cccccccccccc} \cdots & v_{6n-5} & v_{6n-4} & v_{6n-3} & v_{6n-2} & v_{6n-1} & v_{6n} & \cdots & v_{6(N+1)+1} & v_{6(N+1)+2} & v_{6(N+1)+3} & \cdots \end{array} & \\
\begin{bmatrix}
\vdots & & & & & & & & & & & \\
 & c^L_{z,i}+c^R_{z,i} & & (c^R_{z,i}-c^L_{z,i})y_u & & & & & -(c^L_{z,i}+c^R_{z,i}) & & c^L_{z,i}l^L_i - c^R_{z,i}l^R_i & \\
 & & c^L_{y,i}+c^R_{y,i} & (c^L_{y,i}+c^R_{y,i})z_b & & & & & & -(c^L_{y,i}+c^R_{y,i}) & & \\
 & (c^R_{z,i}-c^L_{z,i})y_u & (c^L_{y,i}+c^R_{y,i})z_b & (c^L_{z,i}+c^R_{z,i}){y_u}^2+(c^L_{y,i}+c^R_{y,i}){z_b}^2 & & & & & (-c^R_{z,i}+c^L_{z,i})y_u & -(c^L_{y,i}+c^R_{y,i})z_b & -(c^L_{z,i}c^L_i + c^R_{z,i}c^R_i)y_u & \\
 & & & & \vdots & & & & & & & \\
 & & & & & \vdots & & & & & & \\
 & & & & & & \vdots & & & & & \\
 & & & & & & & \vdots & & & & \\
 & -(c^L_{z,i}+c^R_{z,i}) & & (c^L_{z,i}-c^R_{z,i})y_u & & & & & c^L_{z,i}+c^R_{z,i} & & -c^L_{z,i}l^L_i + c^R_{z,i}l^R_i & \\
 & & -(c^L_{y,i}+c^R_{y,i}) & -(c^L_{y,i}+c^R_{y,i})z_b & & & & & & c^L_{y,i}+c^R_{y,i} & & \\
 & c^L_{z,i}l^L_i - c^R_{z,i}l^R_i & & -(c^L_{z,i}l^L_i + c^R_{z,i}l^R_i)y_u & & & & & c^R_{z,i}l^R_i - c^L_{z,i}l^L_i & & c^L_{z,i}l^{L2}_i + c^R_{z,i}l^{R2}_i & \\
 & & & & & & & & & & & \vdots
\end{bmatrix} &
\begin{array}{c} \vdots \\ v_{6n-5} \\ v_{6n-4} \\ v_{6n-3} \\ v_{6n-2} \\ v_{6n-1} \\ v_{6n} \\ \vdots \\ v_{6(N+1)+1} \\ v_{6(N+1)+2} \\ v_{6(N+1)+3} \\ \vdots \end{array}
\end{array} \tag{A47}
$$

References

1. Narayanan, S.; Mallik, A.K. Free vibration of thin walled open section beams with constrained damping treatment. *J. Sound Vib.* **1981**, *74*, 429–439. [CrossRef]
2. Bank, L.C.; Kao, C.H. Dynamic response of thin-walled composite material Timoshenko beams. *J. Energy Resour. Technol.* **1990**, *112*, 149–154. [CrossRef]
3. Rao, S.S.; Jin, H. Analysis of coupled bending-torsional vibration of beams in the presence of uncertainties. *J. Vib. Acoust.* **2014**, *136*, 051004. [CrossRef]
4. Li, J.; Shen, R.; Hua, H.; Jin, X. Coupled bending and torsional vibration of axially loaded thin-walled Timoshenko beams. *Int. J. Mech. Sci.* **2004**, *46*, 299–320. [CrossRef]
5. Jun, L.; Rongying, S.; Hongxing, H.; Xianding, J. Coupled bending and torsional vibration of axially loaded Bernoulli–Euler beams including warping effects. *Appl. Acoust.* **2004**, *65*, 153–170. [CrossRef]
6. Li, J.; Hua, H.; Shen, R.; Jin, X. Stochastic vibration of axially loaded monosymmetric Timoshenko thin-walled beam. *J. Sound Vib.* **2004**, *274*, 915–938. [CrossRef]
7. Lezgy-Nazargah, M.; Vidal, P.; Polit, O. A quasi-3D finite element model for the analysis of thin-walled beams under axial–flexural–torsional loads. *Thin-Walled Struct.* **2021**, *164*, 107811. [CrossRef]
8. Jrad, W.; Mohri, F.; Robin, G.; Daya, E.M.; Al-Hajjar, J. Analytical and finite element solutions of free and forced vibration of unrestrained and braced thin-walled beams. *J. Vib. Control* **2020**, *26*, 255–276. [CrossRef]
9. Chen, H.H.; Hsiao, K.M. Coupled axial-torsional vibration of thin-walled Z-section beam induced by boundary conditions. *Thin-Walled Struct.* **2007**, *45*, 573–583. [CrossRef]
10. Prokić, A. On triply coupled vibrations of thin-walled beams with arbitrary cross-section. *J. Sound Vib.* **2005**, *279*, 723–737. [CrossRef]
11. Prokić, A. On fivefold coupled vibrations of Timoshenko thin-walled beams. *Eng. Struct.* **2006**, *28*, 54–62. [CrossRef]
12. Chen, H.H.; Hsiao, K.M. Quadruply coupled linear free vibrations of thin-walled beams with a generic open section. *Eng. Struct.* **2008**, *30*, 1319–1334. [CrossRef]
13. Kim, N.I.; Seo, K.J.; Kim, M.Y. Free vibration and spatial stability of non-symmetric thin-walled curved beams with variable curvatures. *Int. J. Solids Struct.* **2003**, *40*, 3107–3128. [CrossRef]
14. Kim, N.I.; Kim, M.Y. Spatial free vibration of shear deformable circular curved beams with non-symmetric thin-walled sections. *J. Sound Vib.* **2004**, *276*, 245–271. [CrossRef]
15. Xu, X.; Carrera, E.; Augello, R.; Daneshkhah, E.; Yang, H. Benchmarks for higher-order modes evaluation in the free vibration response of open thin-walled beams due to the cross-sectional deformations. *Thin-Walled Struct.* **2021**, *166*, 107965. [CrossRef]
16. Wu, J.S.; Chou, H.M. Free vibration analysis of a cantilever beam carrying any number of elastically mounted point masses with the analytical-and-numerical-combined method. *J. Sound Vib.* **1998**, *213*, 317–332. [CrossRef]
17. Wu, J.S.; Chang, B.H. Free vibration of axial-loaded multi-step Timoshenko beam carrying arbitrary concentrated elements using continuous-mass transfer matrix method. *Eur. J. Mech. A/Solids* **2013**, *38*, 20–37. [CrossRef]
18. Liu, X.; Sun, C.; Banerjee, J.R.; Dan, H.C.; Chang, L. An exact dynamic stiffness method for multibody systems consisting of beams and rigid-bodies. *Mech. Syst. Signal Processing* **2021**, *150*, 107264. [CrossRef]
19. Bambill, D.V.; Rossit, C.A. Forced vibrations of a beam elastically restrained against rotation and carrying a spring–mass system. *Ocean Eng.* **2002**, *29*, 605–626. [CrossRef]
20. Lin, H.Y.; Tsai, Y.C. Free vibration analysis of a uniform multi-span beam carrying multiple spring–mass systems. *J. Sound Vib.* **2007**, *302*, 442–456. [CrossRef]
21. Wu, J.S.; Hsu, T.F. Free vibration analyses of simply supported beams carrying multiple point masses and spring-mass systems with mass of each helical spring considered. *Int. J. Mech. Sci.* **2007**, *49*, 834–852. [CrossRef]
22. Yesilce, Y.; Demirdag, O. Effect of axial force on free vibration of Timoshenko multi-span beam carrying multiple spring-mass systems. *Int. J. Mech. Sci.* **2008**, *50*, 995–1003. [CrossRef]
23. Banerjee, J.R. Free vibration of beams carrying spring-mass systems− A dynamic stiffness approach. *Comput. Struct.* **2012**, *104*, 21–26. [CrossRef]
24. Wu, J.J. Free vibration analysis of beams carrying a number of two-degree-of-freedom spring-damper-mass systems. *Finite Elem. Anal. Des.* **2004**, *40*, 363–381. [CrossRef]
25. Wu, J.J. Use of equivalent-damper method for free vibration analysis of a beam carrying multiple two degree-of-freedom spring–damper–mass systems. *J. Sound Vib.* **2005**, *281*, 275–293. [CrossRef]
26. Wu, J.J. Use of effective stiffness matrix for the free vibration analyses of a non-uniform cantilever beam carrying multiple two degree-of-freedom spring–damper–mass systems. *Comput. Struct.* **2003**, *81*, 2319–2330. [CrossRef]
27. El-Sayed, T.A.; El-Mongy, H.H. Application of variational iteration method to free vibration analysis of a tapered beam mounted on two-degree of freedom subsystems. *Appl. Math. Model.* **2018**, *58*, 349–364. [CrossRef]
28. Mei, C. A Wave-Based Analytical Solution to Free Vibrations in a Combined Euler–Bernoulli Beam/Frame and a Two-Degree-of-Freedom Spring–Mass System. *J. Vib. Acoust.* **2018**, *140*, 061001. [CrossRef]
29. Chen, G.; Zeng, X.; Liu, X.; Rui, X. Transfer matrix method for the free and forced vibration analyses of multi-step Timoshenko beams coupled with rigid bodies on springs. *Appl. Math. Model.* **2020**, *87*, 152–170. [CrossRef]

30. Wu, J.S.; Chen, D.W. Dynamic analysis of a uniform cantilever beam carrying a number of elastically mounted point masses with dampers. *J. Sound Vib.* **2000**, *229*, 549–578. [CrossRef]
31. Muscolino, G.; Benfratello, S.; Sidoti, A. Dynamics analysis of distributed parameter system subjected to a moving oscillator with random mass, velocity and acceleration. *Probabilistic Eng. Mech.* **2002**, *17*, 63–72. [CrossRef]
32. Barry, O.; Oguamanam, D.C.D.; Zu, J.W. On the dynamic analysis of a beam carrying multiple mass-spring-mass-damper system. *Shock Vib.* **2014**, *2014*, 485630. [CrossRef]
33. Bukhari, M.A.; Barry, O.R. Nonlinear Vibrations Analysis of Overhead Power Lines: A Beam With Mass–Spring–Damper–Mass Systems. *J. Vib. Acoust.* **2018**, *140*, 031004. [CrossRef]
34. Gupta, S.K.; Malla, A.L.; Barry, O.R. Nonlinear vibration analysis of vortex-induced vibrations in overhead power lines with nonlinear vibration absorbers. *Nonlinear Dyn.* **2021**, *103*, 27–47. [CrossRef]
35. Aasi, A.; Aghaei, S.M.; Panchapakesan, B. Experimental Investigation of Natural Frequency and Forced Vibration of Euler-Bernoulli Beam under Displacement of Concentrated Mass and Load. *Int. J. Aerosp. Mech. Eng.* **2022**, *16*, 103–107.
36. Chen, J.; Dong, D.; Yan, B.; Hua, C. An Analytical Study on Forced Vibration of Beams Carrying a Number of Two Degrees-of-Freedom Spring–Damper–Mass Subsystems. *J. Vib. Acoust.* **2016**, *138*, 061011. [CrossRef]
37. Mei, C. Free and Forced Wave Vibration Analysis of a Timoshenko Beam/Frame Carrying a Two Degrees-of-Freedom Spring-Mass System. *J. Vib. Acoust.* **2021**, *143*, 061008. [CrossRef]
38. Oguamanam, D.C.D. Free vibration of beams with finite mass rigid tip load and flexural–torsional coupling. *Int. J. Mech. Sci.* **2003**, *45*, 963–979. [CrossRef]
39. Gökdağ, H.; Kopmaz, O. Coupled bending and torsional vibration of a beam with in-span and tip attachments. *J. Sound Vib.* **2005**, *287*, 591–610. [CrossRef]
40. Wang, Q.; Wang, Z.; Fan, B. Coupled bending and torsional vibration characteristics analysis of inhomogeneous wind turbine tower with variable cross section under elastic constraint. *Appl. Math. Model.* **2021**, *93*, 188–205. [CrossRef]
41. Wu, J.; Titurus, B. Damping augmentation of a rotating beam-tendon system via internally placed spring-damper elements. *J. Sound Vib.* **2021**, *510*, 116315. [CrossRef]
42. Hoffmeyer, D.; Høgsberg, J. Calibration and balancing of multiple tuned mass absorbers for damping of coupled bending-torsion beam vibrations. *J. Vib. Acoust.* **2020**, *142*, 044501. [CrossRef]
43. Burlon, A.; Failla, G.; Arena, F. Coupled bending–torsional frequency response of beams with attachments: Exact solutions including warping effects. *Acta Mech.* **2018**, *229*, 2445–2475. [CrossRef]
44. Burlon, A.; Failla, G.; Arena, F. Coupled bending and torsional free vibrations of beams with in-span supports and attached masses. *Eur. J. Mech. A/Solids* **2017**, *66*, 387–411. [CrossRef]
45. Burlon, A.; Failla, G.; Arena, F. Exact stochastic analysis of coupled bending-torsion beams with in-span supports and masses. *Probabilistic Eng. Mech.* **2018**, *54*, 53–64. [CrossRef]
46. Burlon, A.; Failla, G.; Arena, F. Exact frequency response of two-node coupled bending-torsional beam element with attachments. *Appl. Math. Model.* **2018**, *63*, 508–537. [CrossRef]
47. Burlon, A.; Failla, G. Flexural wave propagation in locally-resonant beams with uncoupled/coupled bending-torsion beam-like resonators. *Int. J. Mech. Sci.* **2022**, *215*, 106925. [CrossRef]
48. Zhou, J.; Wen, S.; Li, F.; Zhu, Y. Coupled bending and torsional vibrations of non-uniform thin-walled beams by the transfer differential transform method and experiments. *Thin-Walled Struct.* **2018**, *127*, 373–388. [CrossRef]
49. Zhong, H.; Liu, Z.; Qin, H.; Liu, Y. Static analysis of thin-walled space frame structures with arbitrary closed cross-sections using transfer matrix method. *Thin-Walled Struct.* **2018**, *123*, 255–269. [CrossRef]